**Showcasing a literature review from Dr Zhang's laboratory, School of Mechanical and Manufacturing Engineering, University of New South Wales, Sydney, Australia.**
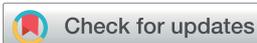
Recent developments of hybrid piezo–triboelectric nanogenerators for flexible sensors and energy harvesters

Hybrid piezo–triboelectric nanogenerators constitute a new class of self-powered systems that exploit the synergy of piezoelectric and triboelectric mechanisms to improve energy harvesting efficiencies and address the energy and power needs of portable and wearable electronic devices. Herein, we review the recent advances of hybrid piezo–triboelectric nanogenerators, with a particular focus on microstructure design, synergy mechanisms, and future research opportunities with significant potential for physiological monitoring, health care applications, transportation, and energy harvesting.

ROYAL SOCIETY
OF **CHEMISTRY**

rsc.li/nanoscale-advances

Check for updates
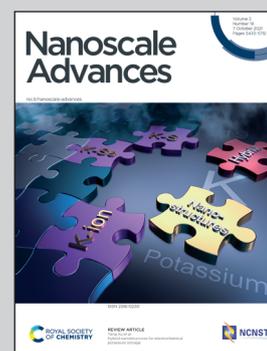
Recent developments of hybrid piezo–triboelectric nanogenerators for flexible sensors and energy harvesters

Jin Zhang, [ID] *[a] Yilin He,[a] Cyrille Boyer, [ID] *[b] Kourosh Kalantar-Zadeh, [ID] [b] Shuhua Peng, [ID] [a] Dewei Chu [ID] [c] and Chun H. Wang [ID] *[a]

Hybrid piezo–triboelectric nanogenerators constitute a new class of self-powered systems that exploit the synergy of piezoelectric and triboelectric mechanisms to improve energy harvesting efficiencies and address the energy and power needs of portable and wearable electronic devices. The unique, synergistic electrical coupling mechanisms of piezoelectric and triboelectric effects increase the electric outputs and energy conversion efficiency of hybrid generators to beyond a linear summation of the contributions from individual triboelectric and piezoelectric mechanisms. Due to their large surface-area-to-volume ratios and outstanding mechanical, electronic and thermal properties, nanomaterials are favourable building blocks for constructing hybrid nanogenerators and represent a large family of flexible energy harvesting electronic structures and devices. Herein, we review the recent advances of hybrid piezo–triboelectric nanogenerators, with a particular focus on microstructure design, synergy

[a]School of Mechanical and Manufacturing Engineering, University of New South Wales (UNSW), Sydney, NSW 2052, Australia. E-mail: jin.zhang6@unsw.edu.au; chun.h.wang@unsw.edu.au

[b]School of Chemical Engineering, UNSW, Building E8, Sydney, Kensington, NSW 2052, Australia. E-mail: cboyer@unsw.edu.au

[c]School of Materials Science and Engineering, UNSW, Building E10, Sydney, Kensington, NSW 2052, Australia

Jin Zhang received her PhD from Deakin University and is currently a Scientia Senior Lecturer at the University of New South Wales, Sydney, Australia. Before joining UNSW, she worked at the Institute for Frontier Materials, Deakin University as a postdoctoral research fellow, the Sir Lawrence Wackett Aerospace Research Centre, RMIT University as a research fellow, and the Australian Future Fibres Research & Innovation Centre as a senior research fellow. Jin received the Endeavour Fellowship from the Department of Industry, Innovation, Science, Research and Tertiary Education (DIISRTE) of the Australian government in 2012 and Victoria Fellowship from the Department of Victorian State Development Business and Innovation in 2013. Her research interests include innovative functional fibres and composites, energy harvesting and actuation, lightweight composite structures, flexible sensors and smart textiles, and 3D printing materials.

Yilin He obtained his Master's degree from the School of Materials Science and Engineering, University of New South Wales, Sydney, Australia and is currently a PhD student in the School of Mechanical and Manufacturing Engineering at UNSW. His current research interest is in the study of energy harvesting materials and structures, and the fabrication and application of nanogenerators (especially triboelectric and piezoelectric based devices).

mechanisms, and future research opportunities with significant potential for physiological monitoring, health care applications, transportation, and energy harvesting. The main strategies for improving electrical output performance are identified and examined, including novel nanostructures for increasing the contact area of the triboelectric pair, and nano-additives for enhancing the surface potential difference between the triboelectric pair and piezoelectric layers. Future applications and commercialization opportunities of these nanogenerators are also reviewed.

Introduction

Flexible electronics, portable and wearable devices have attracted significant interest for research and applications in recent years. Passive sensor systems require batteries as a power source and thus can be inconvenient for many applications due to the need for frequent charging and replacement. What's more, batteries are generally the heaviest and bulkiest components of electronic systems, which also limit portability and inhibit the incorporation of electronic devices into clothing without affecting wearing comfort. An appealing solution is to scavenge and harvest energy from the surrounding environment and to convert waste energy to electrical energy. For example, abundant mechanical energies from human motion,

Cyrille Boyer received his PhD from the University of Montpellier II (Ecole Nationale Superieure de Chimie de Montpellier, France). He pursued his PhD in collaboration with Solvay-Solexis for the preparation of new adhesives, which were tested in industrial scale. At the end of his PhD, he undertook a position with Dupont Performance Elastomers, dealing with the synthesis of fluorinated elastomers. Later, he joined the School of Chemical Engineering at the University of New South Wales, where, in 2009, he was awarded an Australian Research Council Fellowship (ARC-APD). In 2011, he joined the Australian Centre for Nanomedicine as a project leader to develop new polymeric nanoparticles for drug delivery and gene therapy. In 2012, Cyrille was awarded an Australian Research Council – Future Fellowship. In January 2017, Cyrille was promoted as full Professor at the University of New South Wales and co-Director of Australian Centre for Nanomedicine. More recently, he served as Deputy Head of School (research). Cyrille's research interests mainly cover the preparation of functional macromolecules, where he developed new polymerization techniques using photocatalysts. These macromolecules find applications in various areas, including nanomedicine and energy storage. Since 2018, he has been listed as Highly Cited Researcher in Chemistry. Cyrille has published over 325 research articles, including 20 highly cited articles according to the Web of Science and 5 international patents, patented by several companies, including Dupont Performance Elastomers, Toso Company, etc. His publication has attracted over 22,000 citations. The research by his group has been recognized by several research awards, including the 2018 IUPAC-Polymer International Young Researcher award, 2016 ACS Biomacromolecules/Macromolecules Young Researcher Awards, 2016 Journal of Polymer Science Innovation Award, Le Fevre Memorial Prize for Chemistry, 2015 Malcolm McIntosh Prize for Physical Science (one of the six Prime Minister Prizes), etc.*

Kourosh Kalantar-Zadeh is a professor of Chemical Engineering at UNSW and one of the Australian Research Council Laureate Fellows of 2018. He is involved in research in the fields of materials sciences and sensors, has co-authored >450 scientific papers and is also a member of the editorial boards of journals such as ACS Applied Nano Materials, Advanced Materials Technologies, and ACS Nano. *He has received many international awards including the 2017 IEEE Sensor Council Achievement and 2018 ACS Advances in Measurement Science Lectureship awards and also the 2020 RSC Robert Boyle Prize.*

airflow, water waves, and water flow are wasted. If converted to electricity, they can reduce or eliminate the need for batteries, making sensor systems self-powered and providing an effective and green approach to tackling global issues such as the depletion of non-renewable energy resources and inconvenience of battery charging/replacement.[1] Taking human activity as an example, footsteps or arm movement from a typical person (68 kg) can generate kinetic powers of around 67 W and 60 W, respectively, while breathing and finger typing can generate 0.83 W and 6.9 mW, respectively.[2] Current on-body electronics require 200 μW to 1 W, which can be met by scavenging biomechanical energy from human motion.

Since 'piezoelectric vibration-powered microgenerators' were proposed by P. Glynne-Jones in 2001,[3] the concept of nanogenerators was expanded by Z. L. Wang in the early 2000s using piezoelectric zinc oxide (ZnO) nanowire arrays for converting mechanic disturbance from an atomic force microscope to electrical energy.[4] Since then, a tremendous amount of research, based on various nanostructures and nano-architectures, has been reported for converting mechanical

energy to electric energy based on piezoelectric or triboelectric effects. Compared with traditional mechanical energy generators (e.g. hydraulic generators and wind power generators), nanogenerators possess many advantages such as being small scale, low cost, facile fabrication, and portability.[5,6]

The piezoelectric effect refers to the phenomenon that the polarizations of piezoelectric materials change when they are subjected to mechanical stress, either because of the reconfiguration of the dipole-inducing surrounding or the re-orientation of molecular dipole moments, resulting in positive and negative electric center shifts that generate an electric field.[7] The piezoelectric effect can be reversible, i.e., the application of an electrical charge can generate mechanical strain, and can operate in a wide frequency range and many motion modes. Piezoelectric crystals can be conveniently reduced to nanosized fillers that retain the piezoelectricity for the assembly of nanogenerators. Nanofillers include zero-dimensional (0D) materials such as barium titanate (BTO)[8] and potassium sodium niobate (KNN) nanoparticles;[9] one-dimensional (1D) materials such as lead zirconate titanate (PZT) nanofibres,[10] zinc oxide (ZnO) nanorods, gallium nitride (GaN),[11] and indium nitride (InN) nanowires;[12] and two-dimensional (2D) fillers such as tin disulfide (SnS_2)[13] and molybdenum disulfide (MoS_2) nanosheets.[14] Piezoelectric polymers based on polyvinylidene difluoride (PVDF) and their nanocomposites are also predominately used for developing piezoelectric nanogenerators.

By contrast, the triboelectric effect relies on contact-induced electrification when two electrically-charged materials move relatively to each other. This occurs by friction after materials make contact (contact-separate or sliding modes).[15] The polarity of the induced charge is directly related to the relative polarity of the triboelectric pair. Nanomaterials such as 0D nanoparticles (e.g. Ag nanoparticles[16]), 1D nanowires and nanofibres,[17] and 2D nanosheets (e.g. h-BN,[18] metal–organic frameworks (MOFs)[19] and transition metal dichalcogenides (TMDs)[20]) have been utilized to modify electrode or/and triboelectric materials to induce and enhance triboelectricity, by reducing internal resistance, and augment charge generation or supply extra charge trapping sites.[21]

Chun-Hui Wang is currently a professor and Head of the School of Mechanical and Manufacturing Engineering at the University of New South Wales, Sydney, Australia. He leads a research group focused on multifunctional composite materials for sensors, actuators, energy storage, and high-performance structures in extreme environments. He has held leadership appointments in government and university sectors. In addition to authoring 400+ publications, he collaborated with numerous companies to translate his research into practical outcomes. In 2018 he was elected a Fellow of the Australian Academy of Technology and Engineering in recognition of his achievements and leadership in research and impact.

Shuhua Peng obtained his PhD degree in polymer science and engineering from Deakin University. He is currently an ARC DECRA Fellow in the School of Mechanical and Manufacturing Engineering at the University of New South Wales, Sydney. His research covers advanced functional materials for applications such as wearable electronics and sensors, energy harvesting and storage, soft robotics, and surface treatments.

Dewei Chu is a professor at the School of Materials Science and Engineering, The University of New South Wales, Australia. His current research interest is in nanoionic materials for nano-electronic devices.
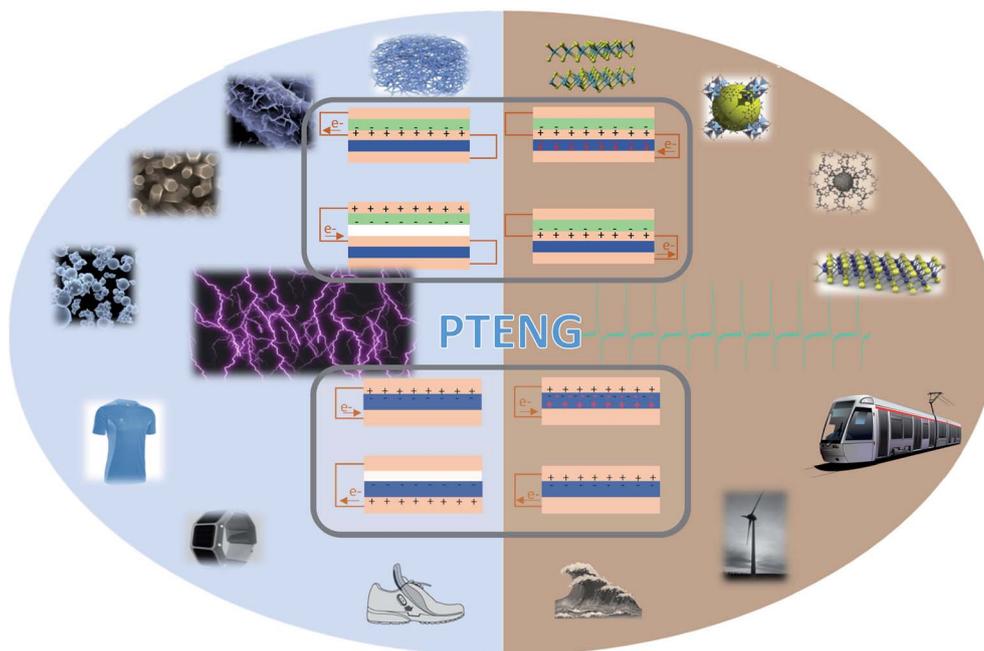
Fig. 1 Schematic illustration of hybrid piezo−triboelectric nanogenerators (PTENGs). The structure design of PTENGs mainly includes three-electrode (top) and two-electrode (bottom) modules. Various nanofillers have been incorporated to generate piezoelectric or triboelectric effects; they can be 0D nanoparticles, 1D nanorods, nanowires and nanofibres, and 2D nanosheets (*e.g.* h-BN, metal−organic frameworks, and transition metal dichalcogenides). PTENGs have broad application in self-powered flexible sensors embedded in clothing and shoes, and large-scale energy harvesters to scavenge wave, wind and motion of transportation vehicles, *etc.*

Although piezoelectric nanogenerators (PENGs) and triboelectric nanogenerators (TENGs) operate under different mechanisms, they can be integrated to enhance the total power output because they both have several common features during mechanical-to-electrical energy conversion. Importantly, both mechanisms work well under mechanical deformation by compression, deflection and vibration. Additionally, the two effects do not overlap during electricity generation since the triboelectrification occurs on the surfaces of materials, while the piezoelectric phenomenon takes place in the bulk below the surface.[22] These features make the hybridization of the PENG and TENG (PTENG) feasible when both mechanical deformation and contact friction of materials occur simultaneously by the rational design of the device structure and polarization direction modulations, increasing energy scavenging and conversion efficiency[23] (Fig. 1). One evident advantage of hybrid PTENG is the increased output current and voltage, which brings great potential for efficiently powering wearable electronic devices.

There is an increasing demand for flexible nanogenerators that can harvest biomechanical energy from human movements such as arm swings, leg motions, heel strikes and elbow joint motion. For wearable technologies, flexibility is an essential performance requirement for wear comfort and the convenience of the wearer. To achieve high flexibility (but not stretchability), thin polymer films or fibrous materials are used as structural constitutes of PTENGs to be able to scavenge energy from a broad range of human movements in low

frequency ranges and to increase their sensitivity and durability as well.[24,25] The present review examines advances in structural designs of flexible PTENGs, the coupling effect between piezoelectric and triboelectric effects, methods for enhancing electrical outputs, their niche applications in practical self-powered sensors and energy harvesters, and challenges for the further development of PTENGs.

Structure design of piezo−triboelectric hybrid nanogenerators

The multifunctionality and performance of hybrid piezo−triboelectric nanogenerators are closely related to their structure design. The structure of PTENGs is mainly divided into two major types: three-electrode modules and two-electrode modules, which are discussed in the following sections.

Three-electrode modules

The strategy of the three-electrode module design is to introduce the piezoelectric and triboelectric functional layers separately. Usually, these layers are separated by introducing an electrode in between, with two triboelectric layers working in the contact-separation mode.[26] Assuming that a dielectric triboelectric layer is in contact with a conductive tribolayer, which doubles as an electrode, to obtain negative charges during compression, the negative and positive piezoelectric charges develop on the upper and lower surfaces of a PTENG shown in Fig. 2a. First, the pre-
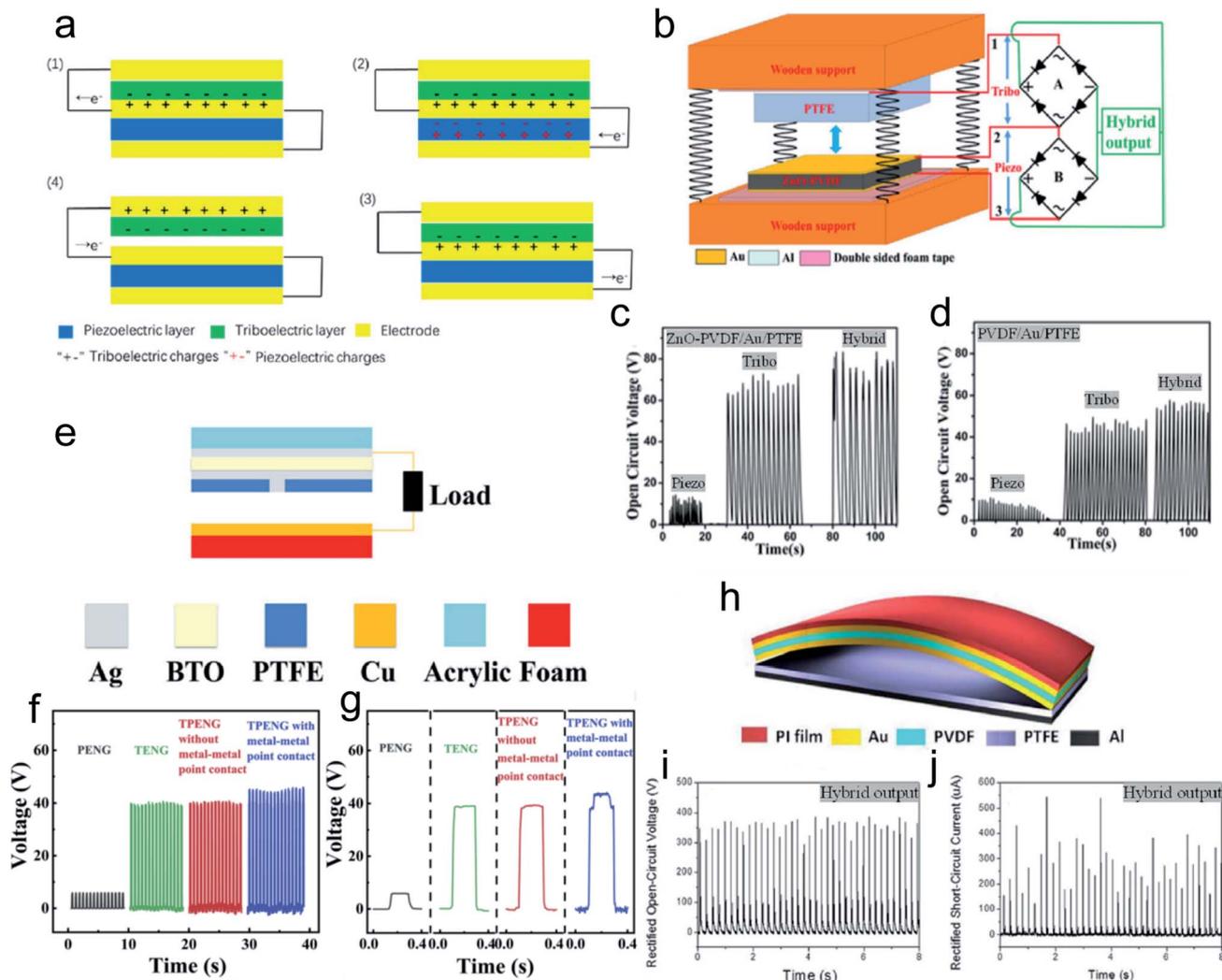
Fig. 2 PTENG with the three-electrode module and the optimized design examples. (a) Working cycle of the three-electrode PTENG. (b) Schematic structure and electro-circuit diagram of a ZnO nanorod/PVDF-PTFE based PTENG. (c) Open-circuit voltage of the PVDF film with ZnO nanorods working under piezo\tribo\hybrid mode. (d) Open-circuit voltage of the PVDF film without ZnO working under piezo\tribo\hybrid mode. Reproduced with permission.[33] Copyright 2018, Elsevier. (e) Schematic structure diagram of a PTENG with point contact between two electrodes. (f) Comparison of the open-circuit voltages for different working modes of the generator and their enlarged view (g). Reproduced with permission.[34] Copyright 2020, Elsevier. (h) Schematic structure diagram of an arc-shaped PVDF-PTFE based PTENG. (i) Open-circuit voltage of the arc-shaped PVDF-PTFE based PTENG. (j) Short-circuit current of the arc-shaped PVDF-PTFE based PTENG. Open access under a Creative Commons Attribution 4.0 International License.[32]

Table 1 Three-electrode PTENG

| Triboelectric constitutes with fillers	Piezoelectric constitutes with fillers	Output voltage	Output current	Output power	Ref.
Silicon rubber with PTFE particles & silicon rubber with silver coated spheres	PZT powder	600 V	17 μA	1.11 W m^{-2}	27
Polydimethylsiloxane (PDMS) & carbon nanotube (CNTs) & graphite nanoparticle	PVDF & carbon nanotube & BTO nanofibre	160 V	—	2.22 W m^{-2}	28
PDMS & graphite nanoparticles	PVDF – trifluoroethylene (PVDF-TrFE) & Ag nanowire	190 V	—	16.46 μW	29
Cellulose paper & MoS$_2$ nanosheet & polyimide (PI)	PVDF nanofibre	50 V	30 nA	0.18 mW cm^{-2}	30
Acrylic & Al	PVDF film	180 V	5.3 μA	127 μW	31
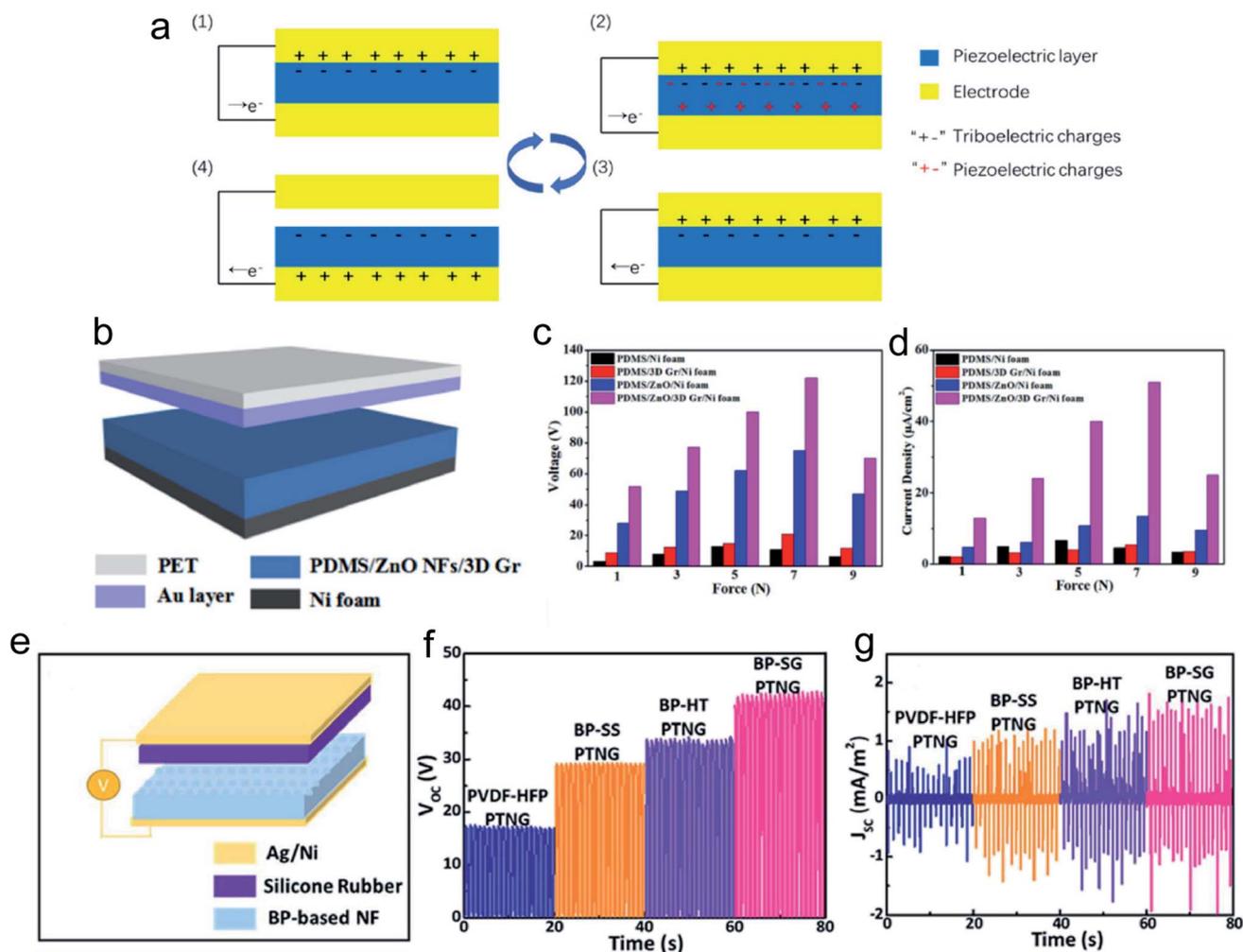
Fig. 3 PTENG with the two-electrode module and examples of the device and performance. (a) Working cycle of a two-electrode PTENG. (b) Schematic structure diagram of a PDMS/ZnO nanoflakes/3D graphene based PTENG. (c) Comparison of the open-circuit voltage under different loads among PDMS/Ni foam, PDMS/3D graphene/Ni foam, PDMS/ZnO nanoflakes/Ni foam, and PDMS/ZnO nanoflakes/3D graphene/Ni foam based PTENGs. (d) Comparison of the short-circuit current under different loads among PDMS/Ni foam, PDMS/3D graphene/Ni foam, PDMS/ZnO nanoflakes/Ni foam, and PDMS/ZnO nanoflakes/3D graphene/Ni foam based PTENGs. Reproduced with permission from ref. 36. Copyright (2018) American Chemical Society. (e) Schematic structure diagram of a BCZT/PVDF nanofibre based PTENG. (f) Comparison of the open-circuit voltage of the PTENG with different enhancements. (g) Comparison of the short-circuit current density of the PTENG with different enhancements. Reproduced from ref. 42 with permission from the Royal Society of Chemistry.

rubbed triboelectric layer and the middle electrode are close to each other until they come into contact. In this process, due to the enhanced electrostatic induction, the positive charges in the upper electrode are attracted to the middle electrode, generating a triboelectric current from the bottom to the top in the upper half of the circuit. Subsequently, the continuous application of compression causes the piezoelectric layer to generate piezoelectric charges. Under electrostatic induction, some of the negative charges in the middle electrode are transferred to the lower electrode, and a corresponding piezoelectric current is generated in the lower half of the circuit. After the pressure is released, the piezoelectric charges disappear. The piezoelectric charges are transferred by electrostatic induction in the lower half of the circuit then flow back to the original location. Simultaneously, a current opposite to the piezoelectric current is generated in the lower half of the circuit. Finally, when the

distance between the triboelectric layer and the middle electrode gradually increases from zero to the maximum, the electrostatic induction between the triboelectric layer and the middle electrode degrades gradually until complete disappearance. The positive charges attracted to the middle electrode by electrostatic induction previously return to the upper electrode, generating a triboelectric current from top to bottom in the upper half of the circuit. Table 1 shows a number of PTENG examples with three-electrode structure consisting of different materials.

For instance, Jung et al. introduced a PTENG with the three-electrode module.[32] In their work, the piezoelectric layer formed the middle layer of a sandwich structure where a layer of gold (Au) was deposited on both surfaces of the piezoelectric PVDF film. The triboelectric layers consist of a polytetrafluoroethylene (PTFE) film and an aluminum (Al) electrode. To utilize the contact-separation operation mechanism, the piezoelectric

PVDF layer was bent and connected to the triboelectric PTFE layer by the edge, creating an arc-shape structure (Fig. 2h). With this design, the hybrid nanogenerator was able to produce an output power of 4.44 mW m^{-2}. Singh *et al.* demonstrated another representative three-electrode module example.[33] They prepared a typical module for the PTENG, which consisted of a PTFE electrification layer, a spacer, and a ZnO nanorod-filled piezoelectric PVDF film functional layer. The schematic of the three-electrode device is illustrated in Fig. 2b and it generates an impressive output power of 250 mW m^{-2}.

The three-electrode design is a simple structure module for PTENGs, and the fabrication of its triboelectric and piezoelectric functional parts almost does not interfere with each other. This structure facilitates the enhancements of piezoelectric or triboelectric properties. However, this separation design requires a shared electrode and sometimes two external circuits are needed to harvest the electricity generated from piezoelectric and triboelectric effects separately, which complicates the packaging and increases the volume of the device.

To mitigate the aforementioned disadvantage, researchers have tried to optimize the three-electrode module structure. Zhu *et al.* reported an innovative design of an all-in-one PTENG with point contact and its adjustable charge transfer by ferroelectric polarization.[34] In their work, the device was assembled as a layer-stacking structure, and the functional layers were arranged following the sequence of a top piezoelectric electrode, piezoelectric layer, bottom piezoelectric electrode, triboelectric layer, spacer, and bottom triboelectric electrode (Fig. 2e). Several holes were drilled into the triboelectric layer to prevent the complete isolation of the lower piezoelectric electrode and the triboelectric electrode. When the device was driven under external force, the upper silver (Ag) electrode, the PTFE film, and the lower copper (Cu) electrode functioned as a normal contact-separation TENG using an external circuit. Once the upper part of the device came into contact with the lower part, with the exertion and release of external force, the piezoelectric charges generated by the BTO (BaTiO$_3$) nanoparticles/PVA sheet transferred between the Ag and Cu electrode junction at the PTFE holes; then the electrostatic balance was achieved through the same external circuit as the triboelectric part.

Two-electrode modules

The two-electrode design is a structure that has only one functional layer but combines both triboelectric and piezoelectric properties; the functional layer being sandwiched between two electrodes. A spacer is usually required between one of the electrodes and the functional layer.[35] Assuming the piezoelectric layer acquires negative charges during friction, and the piezoelectric charge distribution when it is pressed is up negative and down positive, the working cycle of the two-electrode PTENG is divided into four stages (Fig. 3a). First, the upper electrode of the pre-rubbed generator moves close to the piezoelectric layer until they touch each other. During this process, as the electrostatic induction between the piezoelectric layer and the upper electrode gradually increases, positive charges flow from the lower electrode through the external circuit to the upper electrode, generating a triboelectric current from top to bottom in the external circuit. As the applied pressure increases, piezoelectric bound charges are then generated inside the piezoelectric layer due to the piezoelectric effect. Because of the electrostatic induction of the piezoelectric charges, the negative charges in the upper electrode flow to the lower electrode, causing a piezoelectric current from top to bottom in the external circuit. When the pressure is removed, the piezoelectric charge disappears, and the charges generated by the piezoelectric effect in the electrode flow back to its original position to achieve electrostatic balance. This process produces a piezoelectric current in the direction opposite to that of the first piezoelectric current. Finally, when the distance between the upper electrode and the piezoelectric layer increases gradually, the electrostatic induction between them becomes weaker. The excess positive charge flows from the upper electrode to the lower electrode, forming a triboelectric current in the external circuit opposite to the first triboelectric current.

Qian *et al.* recently demonstrated a hybrid nanogenerator prepared from PDMS/ZnO nanoflakes/three-dimensional (3D) graphene heterostructures with a two-electrode structure.[36] In their work, 3D graphene was first deposited on a nickel (Ni) foam by chemical vapor deposition (CVD), and the ZnO nanoflakes were produced on the graphene using the solution growth method. PDMS was then spin-coated onto the ZnO nanoflakes/3D graphene/Ni foam substrate to form the functional layer and the bottom electrode. The hybrid energy harvesters were fabricated by assembling a polyethylene terephthalate (PET)/Au electrode with the functional part (Fig. 3b). The PTENG showed peak-to-peak output voltages up to 122 V and peak-to-peak current densities up to 51 μA cm^{-2}, leading to an ultrahigh power density of 6.22 mW cm^{-2}. Table 2 shows a number of PTENG examples with two-electrode structure with different constituent materials.

Table 2 Two-electrode PTENG

Triboelectric constitute with fillers	Piezoelectric constitute with fillers	Output voltage	Output current	Output power	Ref.
Chitosan & PTFE	Chitosan & BaTiO$_3$ nanorods	247.2 V	36.7 μA cm^{-2}	1568 μW cm^{-2}	37
Nickel/copper-coated PET-conductive fabric & PVDF	PVDF nanofibres	210 V	45 μA	2.1 mW	38
PDMS & multi-walled CNTs & ZnO nanoflower	ZnO nanoflower	400 V	30 μA	—	39
PDMS	Calcium doped BZT powder	550 V	34 μA	23.6 W m^{-2}	40
PDMS	BaTiO$_3$ nanoparticle	280 V	5.6 μA	0.04 mW cm^{-2}	41

Wu *et al.* also fabricated a PTENG based on piezoelectric composite nanofibres and silicone rubber with this two-electrode module.[42] The device was prepared as a four-layer structure (Fig. 3e). Instead of using direct contact of the electrode and tribo layer, a piece of silicone rubber was added between the top electrode and the tribo-piezoelectric function layer as another friction counterpart. The piezoelectric layer of the device was made from a PVDF nanofibre network with $(Ba_{0.85}Ca_{0.15})(Zr_{0.1}Ti_{0.9})O_3$ (BCZT) nanoparticles as fillers. Because the silicone rubber was more electronegative than PVDF, the silicone rubber became negatively charged during the triboelectric process while the PVDF matrix received positive charges. Besides, the poling direction of the PVDF/BCZT composite fibre network was consistent with the charge flow direction of triboelectricity by controlling the direction of the electrical field applied to the BCZT-based PVDF nanofibres during the electrospinning process to increase the output of the hybrid device. The final output power density of this generator reached 162 mW m^{-2}, representing 5.5-fold enhancement in comparison with that of a BTO/PVDF-based composite PTENG.

Piezoelectric and triboelectric coupling effects

The hybridization of the piezoelectric and triboelectric effects does not merely result in a simple summation of their output performance. This has been proved in many previous studies on hybridization between piezoelectric and triboelectric effects. Wang *et al.*[43] reported that during the operation of their hybrid PTENG device, the piezoelectric part generated a peak output power density of 84 mW m^{-2}, which was about 13 times higher than that obtained when the piezoelectric effect acted alone.

This piezoelectric property enhancement was suggested to be a side effect of the triboelectric charge accumulation. In their three-electrode module (Fig. 4c), upon contact between the tribo-layer and the top Cu electrode of the piezo-part, there were positive tribo-charges accumulated on the top Cu electrode. The accumulated tribo-charges created an electrical field in the piezoelectric layer, which affected the polarization of the piezoelectric materials. Thus, when the intrinsic poling direction of the piezoelectric material aligned with the electrical field generated by the triboelectric charges, the overall output of the hybrid device was enhanced and *vice versa*.

Another typical example is given by Hassan *et al.*[44] They presented a hybrid device that combined a ZnSnO$_3$ based PENG and a PDMS based TENG. These two parts were separated by a common Cu electrode. When the PENG worked independently, the peak voltage output was around 6 V. After being hybridized with a TENG, the output voltage increased to 62.5 V.

Finite element modelling (FEM) was conducted by Han *et al.* using COMSOL to analyze the impact of tribo charges on the piezoelectricity of the hybrid generator.[45] In their simulation, a PVDF film was placed on a PDMS substrate and the lower surface of the PVDF film and the upper surface of the PDMS substrate were charged with equivalent opposite charges (positive charges in PVDF and negative charges in PDMS). When the PVDF film was bent to produce a piezoelectric potential with zero surface charge density in the interface, the original piezoelectric potential was 146.2 V. With the increase of surface charge density from 0 to 10 μC m^{-2} and 20 μC m^{-2}, the piezoelectric potential was enhanced to 147.3 V and 153.0 V, respectively. The simulation results were also validated by experimental results, *i.e.* the output voltage increased from 68.4 V to 81.6 V when the substrate changed from Al to PDMS.
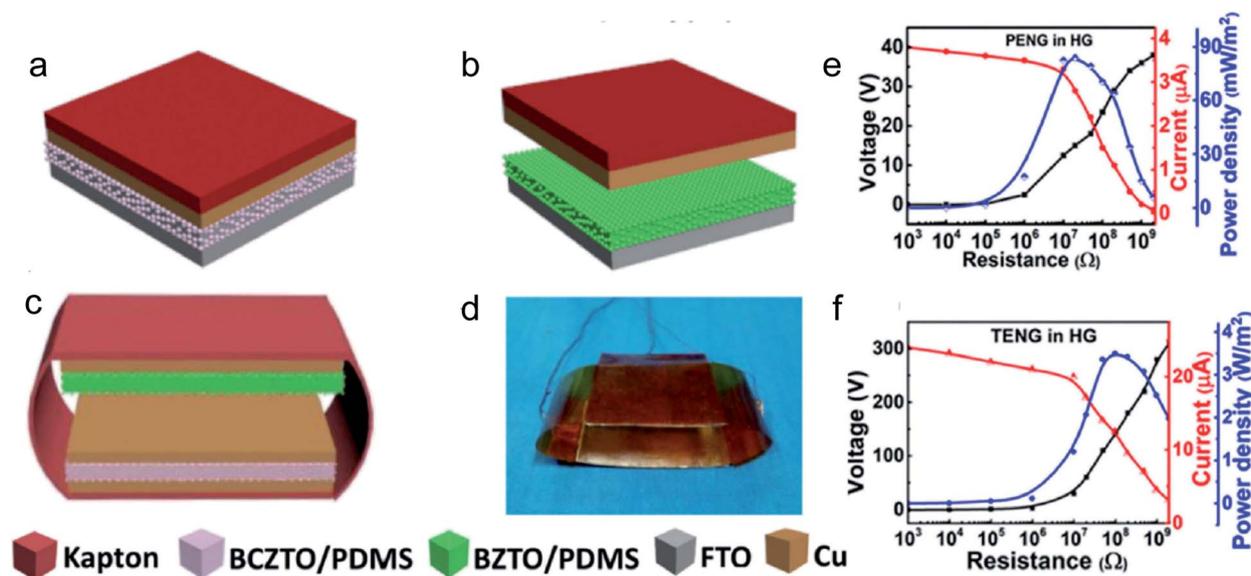

Fig. 4 A PTENG based on the $(Ba_{0.838}Ca_{0.162})(Ti_{0.9072}Zr_{0.092})O_3$ (BCZTO)/PDMS composite and $Ba(Ti_{0.8}Zr_{0.2})O_3$ (BZTO)/PDMS composite. (a–c) Schematic of the piezoelectric part, triboelectric part and hybrid structure. (d) Photo of the BCZTO/PDMS–BZTO/PDMS based PTENG. (e) The output performance of the PENG working under hybrid mode with different loaded resistances. (f) The output performance of the TENG working under hybrid mode with different loaded resistances. Reproduced from ref. 43 with permission of AIP Publishing.
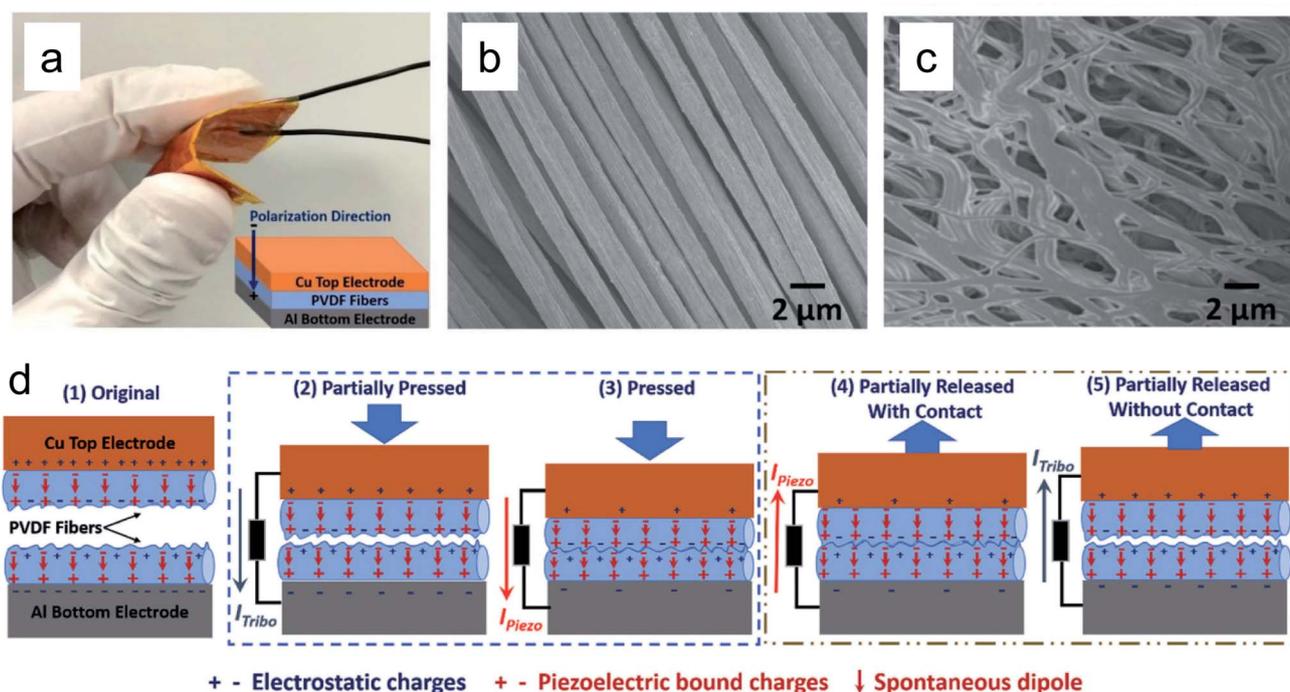
Fig. 5 A PTENG based on aligned electrospun polyvinylidene fluoride (PVDF) fibre mats. (a) Photo and schematic of the PVDF fibre energy harvesting device. SEM image of the bundles of the aligned as-spun fiber (b) and melted at 185 °C (c). (d) Constructive piezoelectric–triboelectric effect in PVDF fibres with aligned electrical polarization. Reproduced with permission.[47] Copyright 2020, John Wiley and Sons.

The triboelectric part of the hybrid nanogenerator is usually fabricated using different types of friction materials, which have dissimilar surface potentials to enable the charge transfer during the triboelectric process. However, it has been proved that when piezoelectric materials like PVDF are directly used as the triboelectric layer or added to the triboelectric layer, the intrinsic dipole moment alters the materials' surface potential. This phenomenon allows the charges to transfer during the contact process, even if the paired materials are the same.[46] Yousry et al. constructed a theoretical module of a two-electrode hybrid nanogenerator using two PVDF fibre mats as both the triboelectric and the piezoelectric layers to address this issue.[47] As shown in Fig. 5d, the two PVDF fibre mats were poled in the

same direction. When the paired PVDF nanofibre mats came into contact and were pressed under external force, opposite piezoelectric charges were generated on the top and bottom surfaces of the two PVDF fibre mats. This effect differentiates the potential of the two contact surfaces of the two PVDF fibre mats so that tribo charge transfer can occur between them.

The above-described mechanism has been employed in the PTENG design to increase the triboelectric output. Narasimulu et al. assembled a PTENG device with multilayers: the top electrode, polyamide 6 (PA6) friction layer, PVDF/ZnSnO$_3$ nanocube/ZnO nanosheet functional layer, and bottom electrode.[48] The PVDF/ZnSnO$_3$ nanocube/ZnO nanosheet layer was regarded as the piezoelectric functional layer and the triboelectric pair with

Table 3 PTENG performance enhancement

| Nanogenerator constitute materials	Enhancement aspect	Enhancement strategies	Output voltage before enhancement	Output voltage after enhancement	Ref.
PDMS & PVDF-TrFE/ 0.78Bi$_{0.5}$Na$_{0.5}$TiO$_3$–0.22SrTiO$_3$ nanofibres	Triboelectricity	Enlarge the contact area: roughen the surface	219 V	253 V	49
Spider silk & PET& PVDF/graphene nanosheets	Triboelectricity	Increase surface potential differences: Adding PVDF	95 V	208 V	50
PVDF/BTO nanoparticles & PA6	Piezoelectricity	Increase the piezoelectric constant: Adding BaTiO$_3$ nanoparticles	384 V	900 V	51
PDMS/ZnO nanoflower/ MWCNT	Piezoelectricity	Increase the piezoelectric charge transfer rate: adding MWCNTs	89.06 V	150 V	39
PDMS/BaTiO$_3$ nanopowder/Ti$_{0.8}$O$_2$ nanosheets/Ag nanoparticles	Piezoelectricity	Increase the piezoelectric constant and charge transfer rate: adding Ti$_{0.8}$O$_2$ nanosheets and Ag nanoparticles	8 V	150 V	52
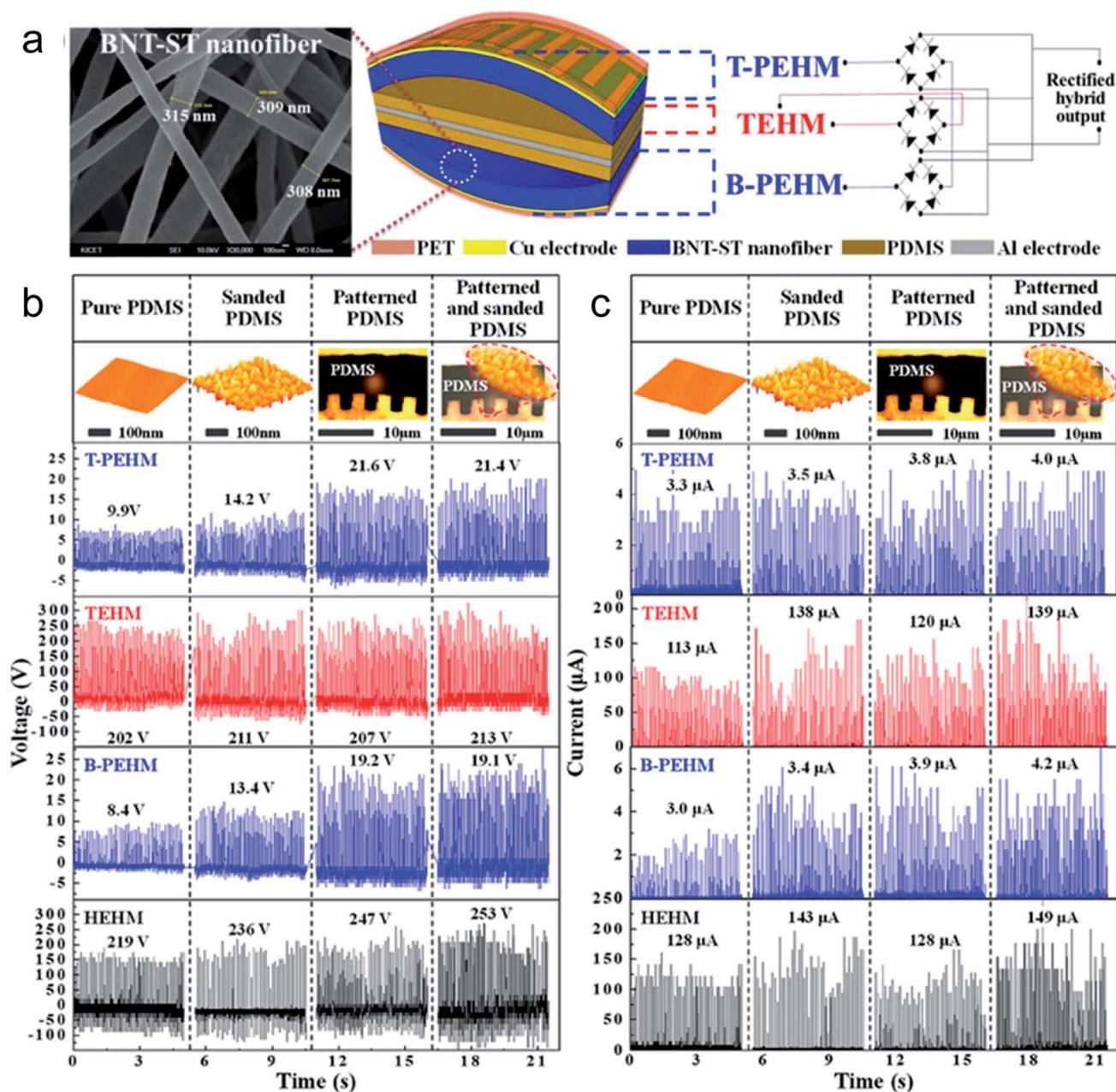
Fig. 6 Modification of surface roughness to improve the electrical output. (a) Schematic of an all-in-one PDMS-PVDF/BNT/ST nanofibre hybrid energy harvester module structure. (b) Output voltage and (c) output current of the PTENG corresponding with the surface roughness of the PDMS layer. Reprinted with permission from ref. 49. Copyright (2020) American Chemical Society.

the PA6 film in this design. During the operation, the negative piezoelectric charges generated by PVDF and ZnO nanosheets resulted in an upper surface potential decrease in the PVDF/ZnSnO$_3$/ZnO film. Thus, the contact surface potential difference between PA6 and PVDF increased, leading to an increase in transferred triboelectric charges during the contact between the PA6 film and the PVDF/ZnSnO$_3$/ZnO film, which therefore significantly improved the triboelectric output. With this piezoelectric charge inducing mechanism, the output power density of the hybrid nanogenerator could significantly increase from 110 mW m^{-2} to 1800 mW m^{-2}.

Piezo−triboelectric nanogenerator output enhancement considerations

Since the hybrid nanogenerator can be regarded as a triboelectric generator and a piezoelectric generator integrated through structural design, technologies used for improving the triboelectric and piezoelectric performance can also be applied to improve the total output performance of the hybrid PTENG (Table 3).
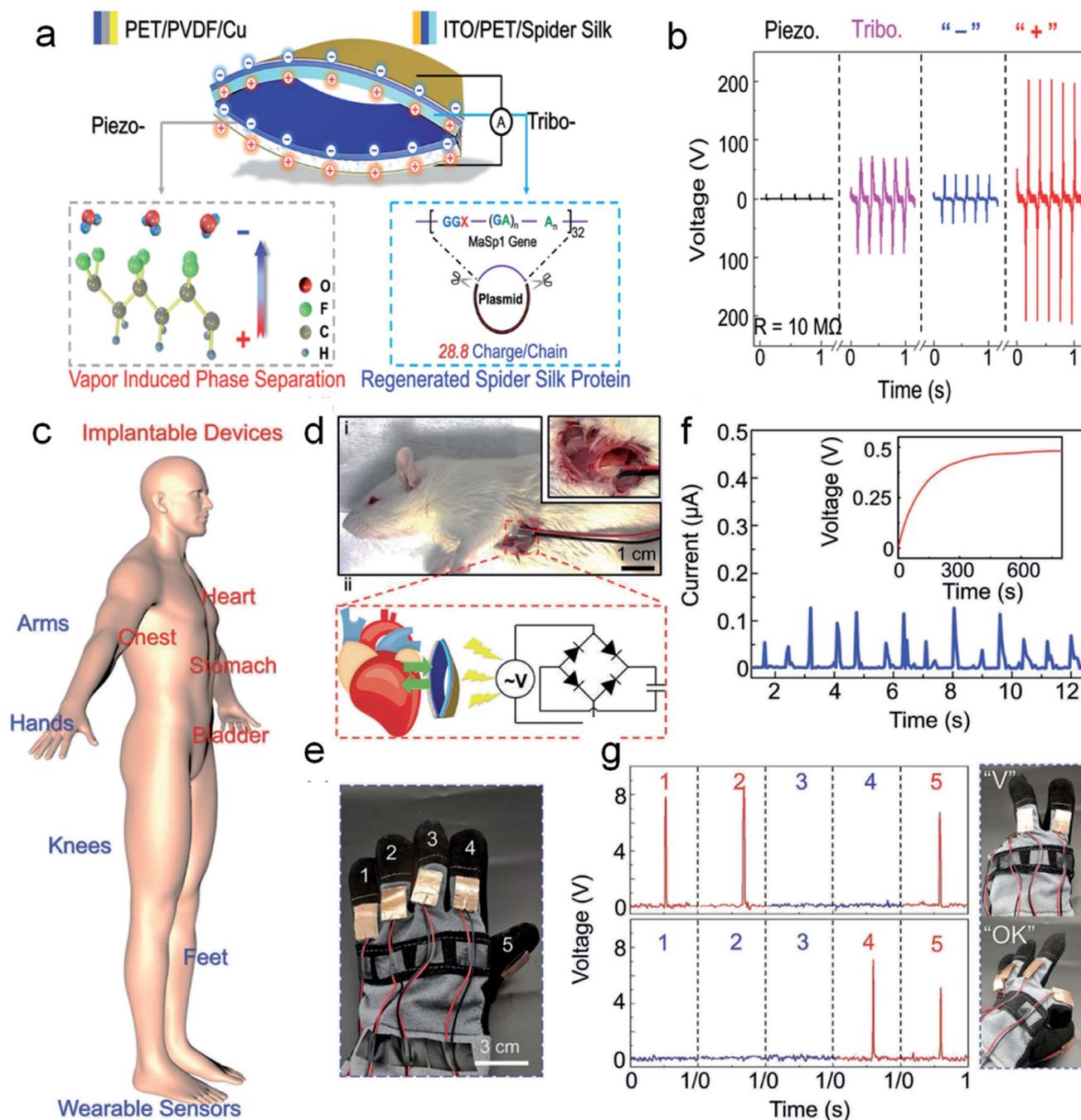
Fig. 7 Biocompatible PTENG with PVDF/graphene decorated PET as the piezoelectric layer and recombinant spider silk coated PET/indium tin oxide (ITO) triboelectric layer. (a) Schematic of structure (b) voltage signals generated by a pure PENG, TENG and PTENG in reverse and forward connection. (c) Demonstration of the PTENG as an implantable and wearable device. (d(i)) Images of the PTENG located on a rat's heart; (ii) schematic of the energy harvesting process from the heart beats of the rat and the circuit connected to the PTENG. (e) Photo of a PTENG-based gesture monitoring glove. (f) Current generated by the PTENG implanted on the rat's heart; the inset shows the voltage−time curve of a capacitor charged by the current collected from the rat heartbeat. (g) Recorded voltage on the five fingers when making "V" and "OK" gestures. Reproduced with permission.[50] Copyright 2020, John Wiley and Sons.

Triboelectric effect enhancement

In a typical contact-separate module (one dielectric layer with two electrodes) TENG, its open-circuit voltage (V_{oc}) and short-circuit current (Q_{sc}) can be represented by the following equations:[53]

$$V_{oc} = \frac{\sigma x}{\varepsilon_0} \tag{1}$$

$$Q_{sc} = \frac{S\sigma x}{d_0 + x} \tag{2}$$

where σ is the triboelectric charge density, x is the distance between the triboelectric layer and the movable electrode, ε_0 is the dielectric constant of the triboelectric layer, d_0 is the thickness of the triboelectric layer, and S is the contact area between the triboelectric layer and the electrode. For a certain triboelectric material, ε_0, σ and d_0 are constants. The distance x varies from 0 to a certain value during the working cycle. Therefore, increasing the contact area S is the simplest and more effective strategy to improve the triboelectric output (short circuit current) and it is usually realized by modifying the surface morphologies of the triboelectric materials.[54] Chen et al. prepared a PTENG that used a silicon template to give the triboelectric layer a pyramidal surface morphology.[55] When the patterned PDMS triboelectric layer was subject to external forces that increased from 5.6 N to 43 N, a more severe deformation of the micro pyramid structure was obtained, and this led to a dramatic output voltage increase from 57 V to 341 V.[56,57]

To improve the triboelectric effect, Yu et al. summarized the main approaches including creating micro/nano structures (to increase the effective triboelectric area, dielectric constant and dipole moment between electrodes), introducing functional groups by chemical modification on friction surfaces (to lead to easy electron gain or loss and charge injection), and modulating the properties of bulk friction materials by dispersing nano-materials (to provide electron trapping sites or enhance dielectric constant) or adding sublayers (as charge storage or transport layers).[58] Zou et al. further reviewed the methods of generating micro/nano surface features by using templating, appending, etching and crumpling techniques.[59] Uniform 3D

patterns such as nanopillars and nanopores can be conveniently created by templates; appending approaches such as coating, electrospinning, 3D printing and block copolymer assembly can increase the surface roughness; laser and plasma etching have also shown to make various surface structures such as nano-bowls, nano-cones and many other features by etching out a part of the surface; the crumpling method attaches friction materials to an elastic material for deforming the surface and producing bumpy morphologies. All these methods have demonstrated increased surface charge density and therefore improved the triboelectric output.

The influence of the surface roughness of the triboelectric layer on the performance of a TPENG was investigated by Ji et al.[49] The micro-scale surface structure was formed by demolding the cured PDMS from a patterned substrate. To achieve a nano-scale surface morphology, the PDMS was sanded with 2000 grit sandpaper for 5 min. Their experimental results showed that creating micro- and nano-morphological structures on the triboelectric layer can effectively improve the electrical output performance of both the triboelectric layer and the piezoelectric layer (Fig. 6). The microstructure was more effective in improving the output performance of the piezoelectric layer, while the nanostructure tended to optimize the output performance of the triboelectric layer. Compared with pure PDMS films, hybrid nanogenerators with both micron and nanometer surface structures exhibited a higher output voltage and output current (253 V and 149 μA, respectively).

Increasing the triboelectric charge density σ can be an effective method to enhance the triboelectric output. This can
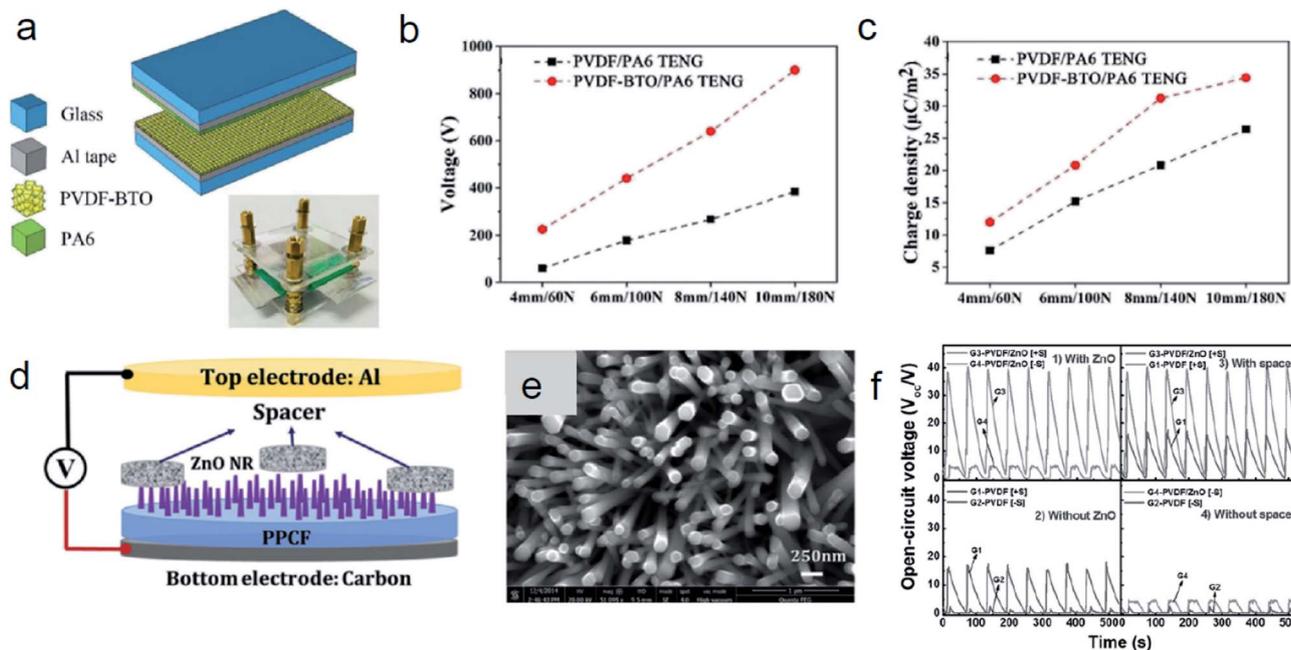

Fig. 8 PTENGs with an enhanced piezoelectric output. (a) Schematic and photo of the BTO nanoparticle/PVDF/PA6 based PTENG. Comparisons of the output voltage (b), and charge density (c) for a PVDF/PA6 PTENG and PVDF–BTO/PA6 PTENG with different spacer distances and force. Reproduced with permission.[51] Copyright 2019, John Wiley and Sons. (d) Schematic of the ZnO/PDMS/PVDF based PTENG. (e) SEM image of the ZnO nanorod arrays. (f) Comparisons of the open-circuit voltage of four types of PTENGs (G1-PVDF with a spacer, G2-PVDF without a spacer, G3-ZnO/PVDF with a spacer, G4-ZnO/PVDF without a spacer). Reproduced with permission.[62] Copyright 2016, John Wiley and Sons.
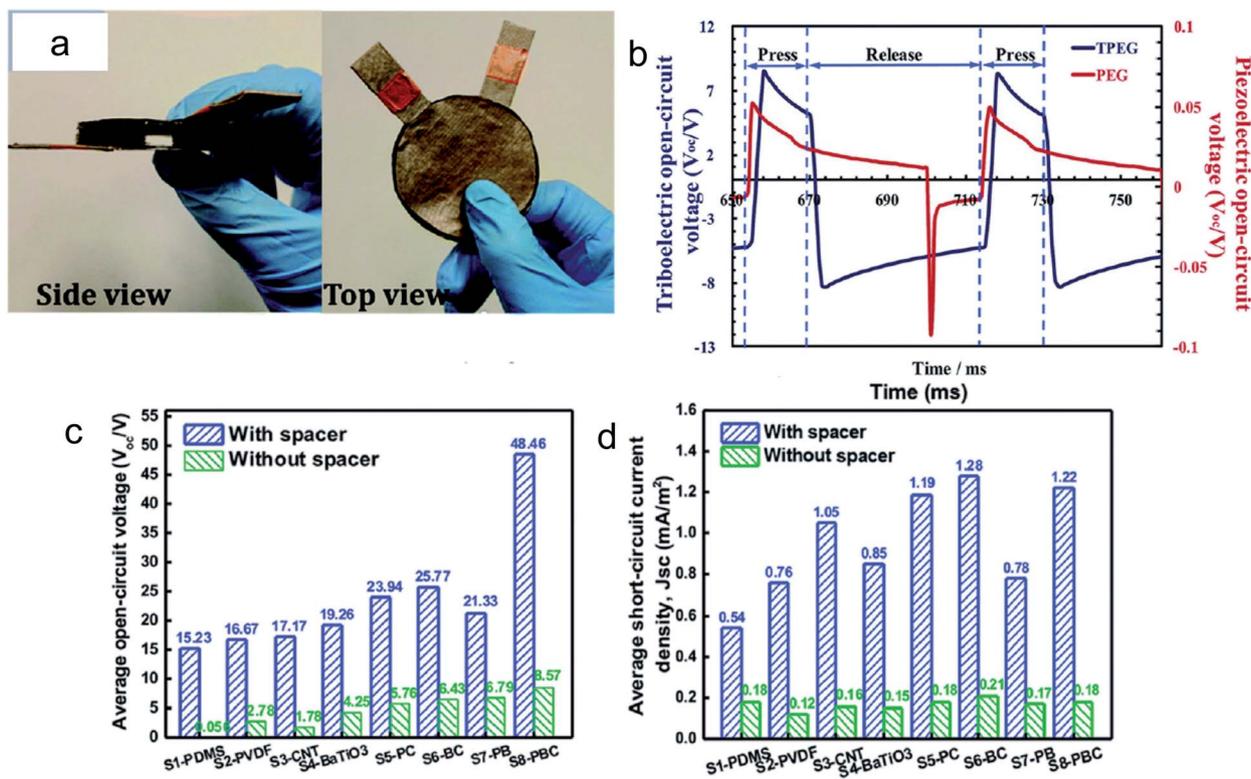
Fig. 9 A flexible PTENG based on polymer/nanofiller and polymer/hybrid nanofiller composites. (a) Side and top views of the hybrid generator. (b) Triboelectric and piezoelectric voltage behavior in one working cycle. (c and d) Open-circuit voltage and short-circuit current of 8 types of generators (functional layer: S1-pure PDMS, S2-pure PVDF, S3-PDMS with CNT, S4-PDMS with BaTiO$_3$, S5-PVDF with CNT, S6-PDMS with BaTiO$_3$ and CNT, S7-PVDF with BaTiO$_3$, S8-PVDF with BaTiO$_3$ and CNT) when working with and without a spacer. Reproduced from ref. 63 with permission from the Royal Society of Chemistry.

be achieved by choosing different triboelectric material pairs with a larger difference in the tribo-series or modifying the triboelectric materials to alter their surface potential. A PTENG based on nitrocellulose nanofibril paper as the triboelectric layer and BTO nanoparticle/MWCNTs@bacterial cellulose paper as the piezoelectric layer was made by Li et al.[60] Wood cellulose paper was treated with HNO$_3$ and H$_2$SO$_4$ to acquire the –NO$_3$ group. In general, cellulose is slightly tribopositive in the triboelectric series because of its excess oxygen atoms and a small amount of hydroxyl groups. With the introduction of the –NO$_3$ group, cellulose has a strong electron-withdrawing ability, which alters its triboelectric properties to tribonegative. The triboelectric and piezoelectric power densities of this hybrid generator reached 10.6 μW cm^{-2} and 1.21 μW cm^{-2}, respectively, by selecting nitrocellulose and nickel as triboelectric pairs and adding a piezoelectric layer composed of BaTiO$_3$ nanoparticles, MWCNTs, and bacterial cellulose.

A PTENG with a recombinant spider silk protein-based tribo layer and piezoelectric PVDF-enhanced PET counter layer[50] was developed by Huang et al. Spider silks were genetically engineered to increase the surface potential difference from PET, so a stronger triboelectric effect was achieved. Furthermore, the PET was attached to a PVDF/graphene film so that the piezo charges generated by PVDF during the working process changed the surface potential of PET and therefore enhanced the

triboelectric charge generation (Fig. 7). In this work, the TENG and PENG were integrated by a 'self-matched' architecture and due to the surface-potential match, the piezoelectric effect in the PENG could induce a higher triboelectric output. The device achieved a maximum power density value of 4 W m^{-2} which was about 100 times that of PENGs with PVDF or its composites as piezoelectric layers.

Piezoelectric effect enhancement

The piezoelectric output can be effectively improved by increasing the piezoelectric constant of the piezo-function part, which is usually realized by adding piezoelectric nanomaterials with high piezoelectric properties to the piezoelectric functional matrix. Xiang et al. constructed a PTENG using a BTO nanoparticle (10 wt%) enhanced PVDF film and PA6 as the functional layers.[51] With the introduction of BaTiO$_3$ nanoparticles, the peak voltage increased from 384 V to 900 V and the charge density increased from 26.4 μC m^{-2} to 34.4 μC m^{-2} (Fig. 8b and c). Chowdhury et al. introduced surface modified lithium doped zinc oxide nanowires and MWCNTs into PVDF as a piezoelectric film for a PTENG.[61] The surface modification was shown to improve the piezoelectric effect, because it reduced the chance of surface dielectric hindrance. The peak output voltage reached 60 V and the peak current reached 75 μA.

Zinc oxide nanorod arrays have been grown directly onto the PDMS/PVDF composite film for performance enhancement by Yang and Daoud.[62] Before the growth of the ZnO nanorod array, the substrate was ultraviolet (UV) treated to enhance the hydrophilicity. The ZnO seed solution was spin-coated onto the as-prepared substrate, and the hydrothermal growth of the ZnO nanorod was followed. The generator was assembled as a two-electrode module (Fig. 8d). The comparison between the open-circuit voltages of the devices with or without ZnO nanorod arrays showed a 21.8 V enhancement, which confirms the positive role of the interfacial ZnO nanorod array in enhancing the output performance of the PTENG by increasing the effective contact area and enhancing contact electrification charges.

Nanomaterials without piezoelectric properties can also be employed to enhance the piezoelectric effect of hybrid nanogenerators. As illustrated in the work by Xue *et al.*',[54] piezoelectric BTO nanoparticles easily became aggregated or chained in the PDMS matrix. MWCNTs with a large aspect ratio could form a long-conduction channel and introduce a bridging effect between the $BaTiO_3$ chains or aggregates. Thus, the electrical conductivity of the piezoelectric substrate was enhanced so that some of the internal piezoelectric charges could be transferred to the surface of the material, improving the electrostatic induction on the surface of the material. As a result, the increased piezoelectric output is achieved.

Yang and Daoud carried out analysis of synergetic effects in a composite-based flexible hybrid generator.[63] The device was fabricated with the two-electrode module, and the test results are presented in Fig. 9. The open-circuit voltage and short-circuit current of PVDF/BTO nanoparticle samples without CNTs are 16.67 V and 0.76 mA m^{-2}, and 19.26 V and 0.85 mA m^{-2}, respectively. With the addition of CNTs, these properties increased to 23.94 V and 1.19 mA m^{-2}, and 25.77 V and 1.28 mA m^{-2}. The spacer could distinguish the triboelectric and piezoelectric potentials and act as a 'charge splitter' during the operation of the hybrid NG. As can be seen in Fig. 9c and d, the group with the spacer yielded a much higher electrical output than the PENG with individual effects made from the same materials.

It has been proved that conductive materials such as Ag[64] and graphene[65] have similar effects to CNTs on the enhancement of piezoelectric performance. These conductive fillers facilitate a more efficient transfer of internal piezoelectric charges to the surface, generating more induced charges on the electrode and increasing the output signal. A typical example is shown in the work by Sriphan *et al.*,[52] where the synergistic effect of adding additional piezoelectric and conductive materials on the PTENG output was studied. In their PDMS composite based PTENG, BTO nanoparticles are the primary piezoelectric ceramic material, Ag nanoparticles improve the conductivity, and $Ti_{0.8}O_2$ nanosheets were used as the secondary piezoelectric material. The electrical testing results confirmed that a small amount of additional piezoelectric ceramics and conductive materials produced more electric dipoles in the composite film, leading to a higher electric output. Specifically, 0.3 vol% of $Ti_{0.8}O_2$ nanosheets and 1.5 vol% of Ag nanoparticles showed the optimum modifying results

with the output voltage and current density reaching 150 V and 0.32 μA cm^{-2}, respectively, which are 60 and 32 times higher than that of neat PDMS-based energy harvesting materials. When the doping ratio of $Ti_{0.8}O_2$ nanosheets reached 0.5 vol%, a higher level of agglomeration of BTO and $Ti_{0.8}O_2$ nanofillers was caused, resulting in a decrease in the generated electrical output.

Applications of hybrid PTENGs

To meet the ever-increasing demand in energy supply, hybrid PTENGs can be conveniently applied as sustainable resources for various purposes, when the waste energy occurs as periodic kinetic energy, whether it is from the movement of waves or wind, or human body motion. Flexible hybrid PTENGs provide direct and active linkage/triggering of the electrical output signals upon external mechanical deformation, and have strong potential for the utilization in self-powered sensors, intelligent human–machine interactions, and energy harvesting devices even for ocean environments (Table 4).[66] The fabrication of PTENGs is generally simple and cost effective and can be easily applied for large-scale productions. Simultaneously, they offer excellent durability and stability, which can be further integrated into the design of smarter and more sophisticated electronic devices.

Self-powered sensors

One of the applications of hybrid nanogenerators is in sensors for bio-detection. By selecting biocompatible flexible materials, hybrid nanogenerators can be developed and attached to different parts of the human body such as the wrist, neck, and joints, which can convert the pulse, swallowing, and joint movements into electrical signals. Collecting and processing these signals and connecting them to medical systems can help in reducing the risk of cardiac arrest, choking in the trachea, or joint diseases, by allowing their real-time monitoring.[55]

Instead of directly attaching to the human body, flexible PTENGs can also be integrated into fabrics and clothing. Guo *et al.* prepared a PTENG based on electrospun PVDF nanofibres that can be sewn onto clothes and trousers to respond to vibration and shock.[67] In their work, once a micro signal generator was connected to the PTENG and the voltage output exceeded a set threshold, the signal generator could send an emergency signal to a terminal through their designed network. In other applications, real-time responses can be used for monitoring falls and other accidents for health care. By considering the amplitude of the signal, PTENGs can then be used as gesture sensors for disease diagnosis, physical therapy and health monitoring.[74] The energy scavenged from the body movement can also be converted into electricity and stored to supply power for these wearable sensors.[75] Fig. 10 shows recent examples of PTENGs based on biopolymer chitosan with high output performance and textile hybrid PTENGs with moisture management capability for wearing comfort. By adopting three enhancement strategies, *i.e.* addition and dispersion of lead-free piezoelectric nanorods (BTO nanorods), using soft

Table 4   Applications of PTENGs

Capabilities and applications	Triboelectric constitutes	Piezoelectric constitutes	Sensitivity	Output voltage	Output power	Ref.
Monitor vital signs such as respiration and pulse / Detect body motion	PDMS & skin	PVDF-TrFE nanofibres	7.84 V N⁻¹ (TENG)	—	84 µW cm⁻² (TENG)	55
Detect body motion / Send alarms to remote terminals	Silk/PEO nanofibres	PVDF nanofibres	1.42 V N⁻¹ (PENG)	500 V	0.11 µW cm⁻² (PENG) / 310 µW cm⁻²	67
Monitor acceleration and brake / Send acceleration signals to remote terminals	Eco flex & nickel fabric	PZT	15 V g⁻¹ (TENG)	—	6.5 mW (PENG)	68
Monitor motion type / Monitor pulse	PDMS film	PZT nanofibres/PVDF-TrFE nanofibres	15.43 V kPa⁻¹ (0–100 kPa) / 18.96 V kPa⁻¹ (100–800 kPa)	—	—	69
Detect vibration and acceleration	Silicone rubber, micropatterned	PVDF film	3.65 µW g⁻¹ (amplitude 3 mm) / 6.14 µW g⁻¹ (amplitude 6 mm)	25.8 V		55
Harvest walking, running and jumping energy / Detect foot pressure	Poly(3,4-ethylenedioxythiophene) (PEDOT) polystyrenesulfonate (PSS) coated fabric	PZT chip	0.228 V N⁻¹	—	1.71 mW	70
Convert low frequency rotation energy to electricity	Steel & PTFE	PVDF	—	51.6 V	1.04 W	71
Power small electronic devices	PDMS & Ag nanoparticles	BTO nanoparticles & Ti$_{0.8}$O$_2$ nanosheets (dispersant)	—	150 V	48 µW cm⁻²	52
Power small electronic devices / Harvest water wave energy	PET-ITO & Cu-Kapton / Kapton & PDMS	PVDF-TrFE nanofibres	—	96 V (PENG) / 88 V (upper TENG) / 361.27 V (lower TENG)	22.18 µW (PENG) / 28.67 µW (upper TENG) / 441 µW (lower TENG)	72
Harvest wind energy in a broad wind speed range	Fluorinated ethylene propylene(FEP) & polyimide & Al	0.67Pb(Mg$_{1/3}$Nb$_{2/3}$)O$_3$–0.33PbTiO$_3$ nanofibres	—	216 V	0.24 mW	73

electrodes based on bacterial cellulose/CNT composites, and using a self-charge pumping module, the electrical outputs of the PTENG based on chitosan/BTO nanorod composite (Fig. 10a) realized an open-circuit voltage of 247.2 V, current density of 36.7 μA cm^{-2}, and peak power density of 1568 μW cm^{-2} (Fig. 10b and c), respectively.[37] The power output increased 4 times over that of neat chitosan TENGs. As shown in Fig. 10d, the powerful nanogenerator successfully lit 100 LED lights and drove 7-segments. For wearable electronics, textile PTENGs based on electrospun PVDF-TrFE nanofibres exhibited a peak power density of 5.2 W m^{-2} at low frequency movement as well as outstanding thermal-moisture management capability (Fig. 10e).[76] These e-textiles have demonstrated to be conveniently embedded into shoe insole or sewn into clothing to power minute electronic devices for motion sensing (Fig. 10f–j).

PTENGs can also be used as self-powered accelerators for various applications such as harsh environment monitoring and wireless sensor nodes. For instance, Wang et al. developed a PZT piezoelectric bimorph that was sandwiched between two TENGs.[68] The TENG parts of the device could respond to vibration corresponding with the attached equipment acceleration, thus generating a triboelectric signal to reflect the acceleration direction and strength. Here the PENG part was connected to the microcontroller unit and radiofrequency transceiver to supply energy so that the triboelectric signal could be sent to a remote terminal to realize remote monitoring. This device showed potential for various machine/robot monitoring applications in harsh environments and remote areas by revealing vibration incidents when unusual acceleration values were found. Due to their high sensitivity to vibration, PTENGs can be made into a self-driving sound recording device or used
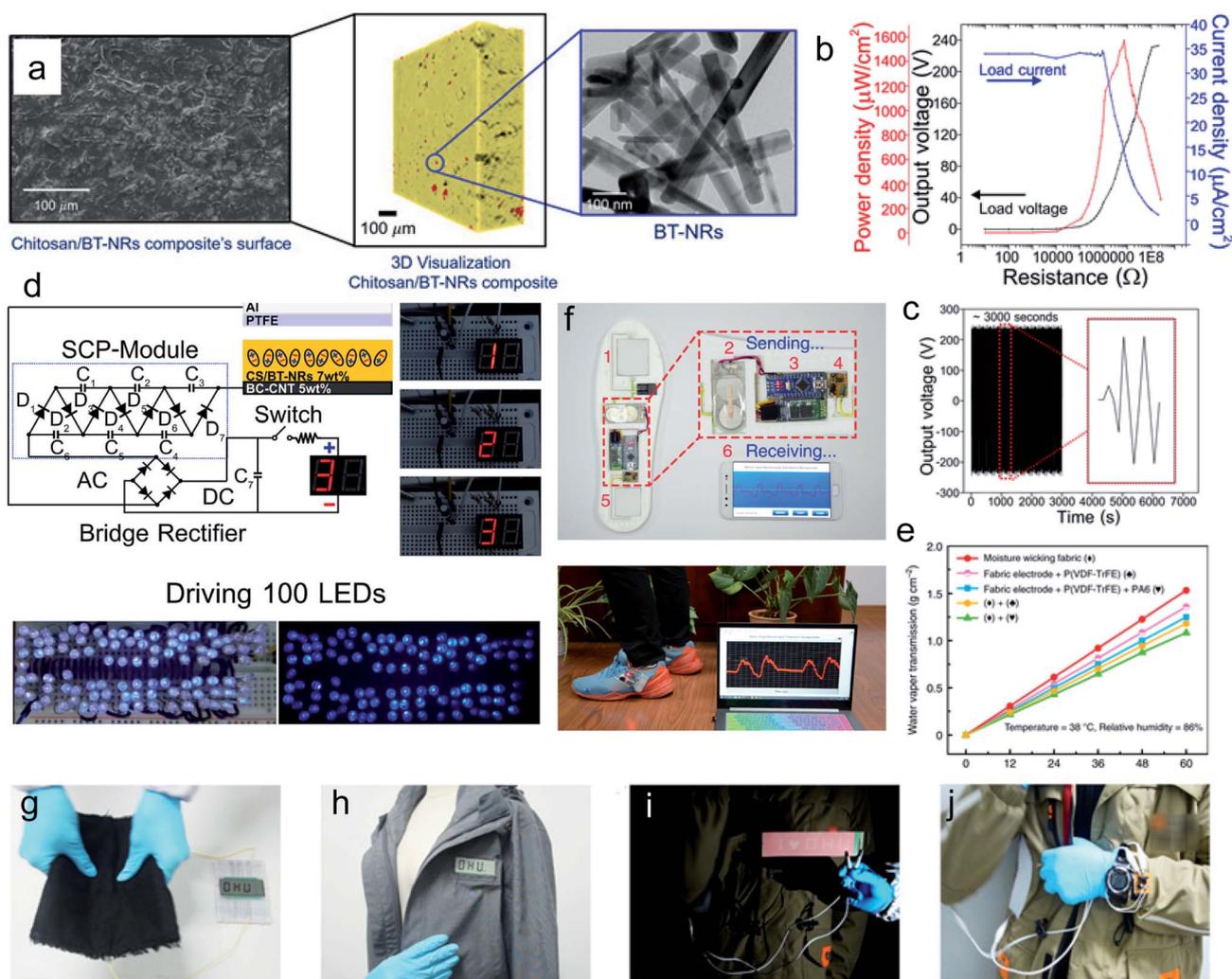

Fig. 10 Flexible PTENGs with high output performance and comfortability for physiological signal monitoring. (a) Morphology of the chitosan/BTO nanorod composite (SEM image of the surface, 3D visualization, and the TEM image of nanorods); (b) high output power and voltage; (c) output voltage stability; (d) driving 100 LEDs and 7-segments. Reproduced with permission.[37] Copyright 2021, Elsevier. (e) Textile PTENG with moisture transmission properties; (f) self-powered gesture sensor printed on shoe insoles for capturing gait while transmitting to a computer in situ; E-textile (g) sewn into fabrics; (h) sewn into clothes to power LCDs; (i and j) sewn onto the surface of clothes to drive digital electroluminescent lattices and watches by scavenging energy from the shoulder movement. Open access under a Creative Commons Attribution 4.0 International License.[76]

for detecting the sound volume and tackle noise issues.[77,78] A PTENG vibration sensor can also be placed on vehicles or lathes, which generate mechanical vibrations, to monitor whether the engine of the vehicle and the rotating shaft of the lathe are working normally, and avoid the danger and loss caused by abnormal vibration. Hybrid PTENGs can also be combined with self-powered gas sensors for hazardous gas detection in harsh environments such as mining sites, chemical factories and industrial tunnels.[79]

Energy harvesters at different scales

Because of the power output limitation, most single PTENGs are designed to harvest micromechanical energy for powering small and portable electronics rather than large instruments. For this end use, PDMS, PVDF, PTFE, and other biocompatible, flexible materials are usually used as the substrate, filled with BTO, KNN, ZnO and other piezoelectric ceramic nanomaterials to prepare functional films or fibres, and are then combined with flexible electrodes such as conductive organic compounds, and conductive fabrics to fabricate wearable devices.[40,80,81] When PTENGs are used for collecting the redundant mechanical energy generated by the human body to supply energy, e.g. for small wearable devices, such minute devices can be integrated with insoles, socks, gloves, pants, or patches that can be attached to flexible surfaces.[70,82] Using current technologies, these wearable PTENGs can produce enough power to drive certain small sensors or charge mobile phones slowly.[22]

What's more, hybrid PTENGs can even be utilized to harvest environmental mechanical energy such as ocean waves and raindrops for self-powered navigation.[83] Chen et al. fabricated
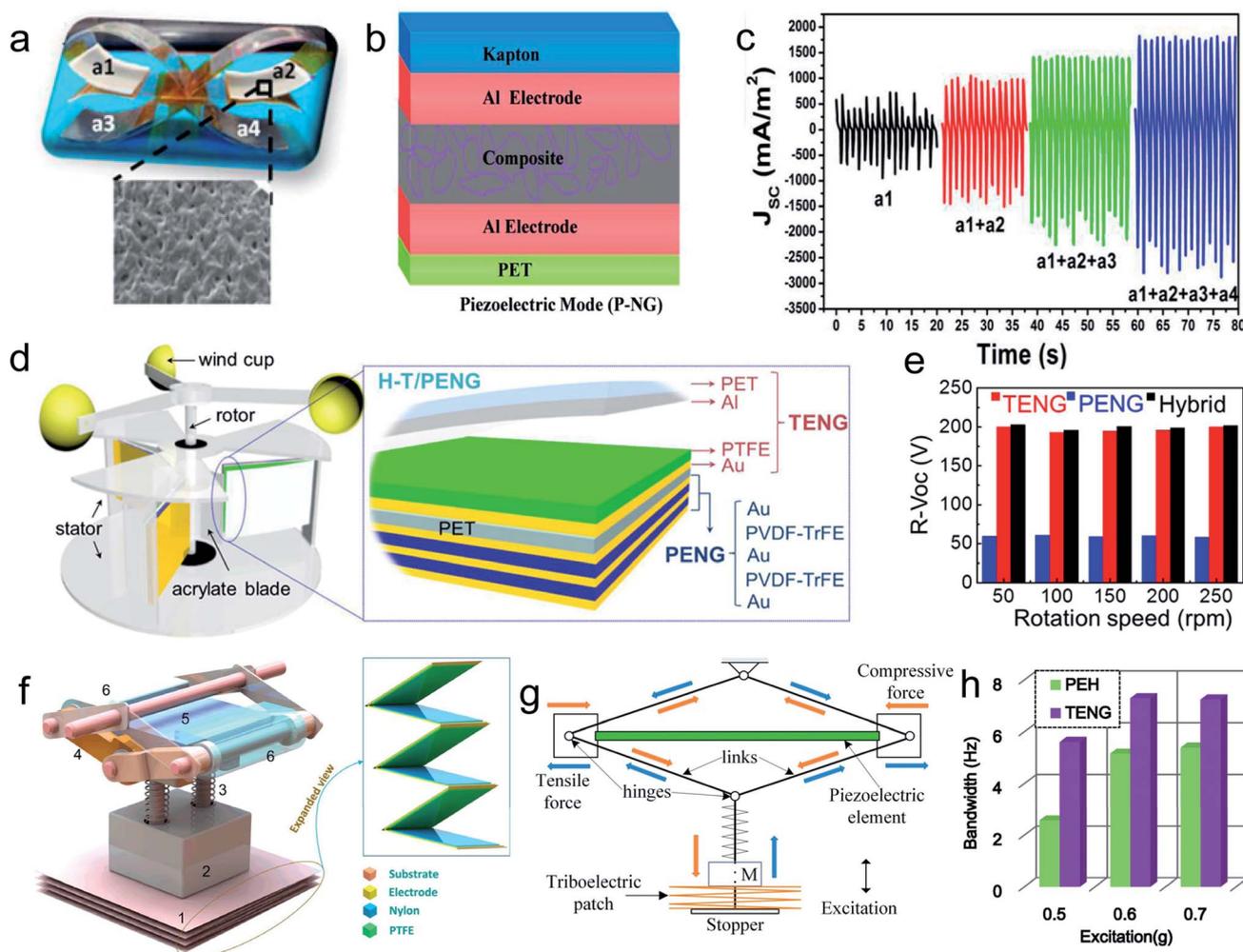

Fig. 11 PTENG energy harvesters with various structural designs. (a) Butterfly wing structure composed of four arc-shaped hybrid nano-generators with an irregular surface morphology (a1, a2, a3, and a4); (b) schematic diagram of PTENG lay-up; (c) output current density of single (a1) and multiunit hybrid nanogenerators connected in parallel at a constant acceleration speed of 1 m s⁻². Reproduced with permission.[84] Copyright 2018, American Chemical Society. (d) Schematic diagram of a PTENG mounted in a custom-built frame for rotational energy harvesting. The PTENG constituting layers are shown in the inset; (e) the rectified open-circuit voltage of a TENG, PENG and PTENG produced at different rotation speeds. Reproduced with permission.[85] Copyright 2019, Elsevier. (f) Structural design of a PTENG for vibration energy harvesting consisting of a spring-mass system; (g) loading condition of the NG; (h) bandwidth of the piezoelectric energy harvester (PEH) and the TENG. Reproduced with permission.[86] Copyright 2018 Elsevier.

a PTENG with a wavy structure, where compliant PVDF-TrFE nanofibres were used as the middle piezoelectric layer; Cu-Kapton was paired with PDMS and PET to form the lower and upper wavy shape triboelectric layers.[72] The wavy structure was self-recoverable due to the flexibility and elasticity of PET, PDMS, and Kapton. These merits make the hybrid nanogenerator more effective in collecting low-frequency mechanical energy with a small amplitude, granting them adaptability for collecting water wave energy, tidal energy, and other types of energy that are difficult to harness using traditional generators.[83] Fig. 11 shows the various structural designs of PTENGs for energy harvesting. Fig. 11a–c present a butterfly wing structure of a multiunit arc-shaped PTENG device that produces current density as high as 2500 mA m^{-2}, mainly resulting from the high surface charge density from the synergistic effect of triboelectric PDMS and Al layers and the piezoelectric $0.3Ba_{0.7}Ca_{0.3}TiO_3$–$0.7BaSn_{0.12}Ti_{0.88}O_3$ (0.3BCT–0.7BST) nanoparticles. Fig. 11d and e show an example of combining a bimorph-based PENG and TENG for efficient rotation-energy collection. The high electrical outputs have shown to be stable and independent of the rotation rate. This uniquely structured PTENG has potential to power electronics in a sustainable manner. Fig. 11f–h show an example of a hybrid PTENG composed of a compressive mode PENG and a TENG to effectively harvest vibration energy at low frequency excitation. The

impact type electric generator exhibited a high power output and a broad operational bandwidth, which facilitates operation in real environments where the frequency varies making the PTENG more adaptable.

Fig. 12 shows a number of application examples where PTENGs are used for self-powered sensors and energy harvesting at different scales. Fig. 12a–c show an example of utilizing PTENG to convert walking or running energy to electricity in order to light up LEDs embedded in shoe soles and to sense foot pressure through wireless transmission.[75] In this work multiple hybrid PTENGs were made to sense different pressure points at forefoot, heel and arch locations. Wang et al. proposed a synergetic piezoelectric and triboelectric mechanism for wind energy harvesting.[73] In their wind driven PTENG module (Fig. 12d and e), the piezoelectric part worked in the vibration area and started to function at low wind speeds, whereas the triboelectric part worked at the vibration boundaries and cooperated with the piezoelectric part at high wind speeds. The vibration of the cantilever in the middle of the generator was caused by the wind, and the cantilever came into contact with or separated from the triboelectric layers on both sides to generate triboelectricity. Different from traditional wind turbines, this PTENG wind harvester could generate electricity at both high and low wind speeds. Moreover, these units offer the advantages of small volume, low cost, and easy maintenance. Wang et al. recently
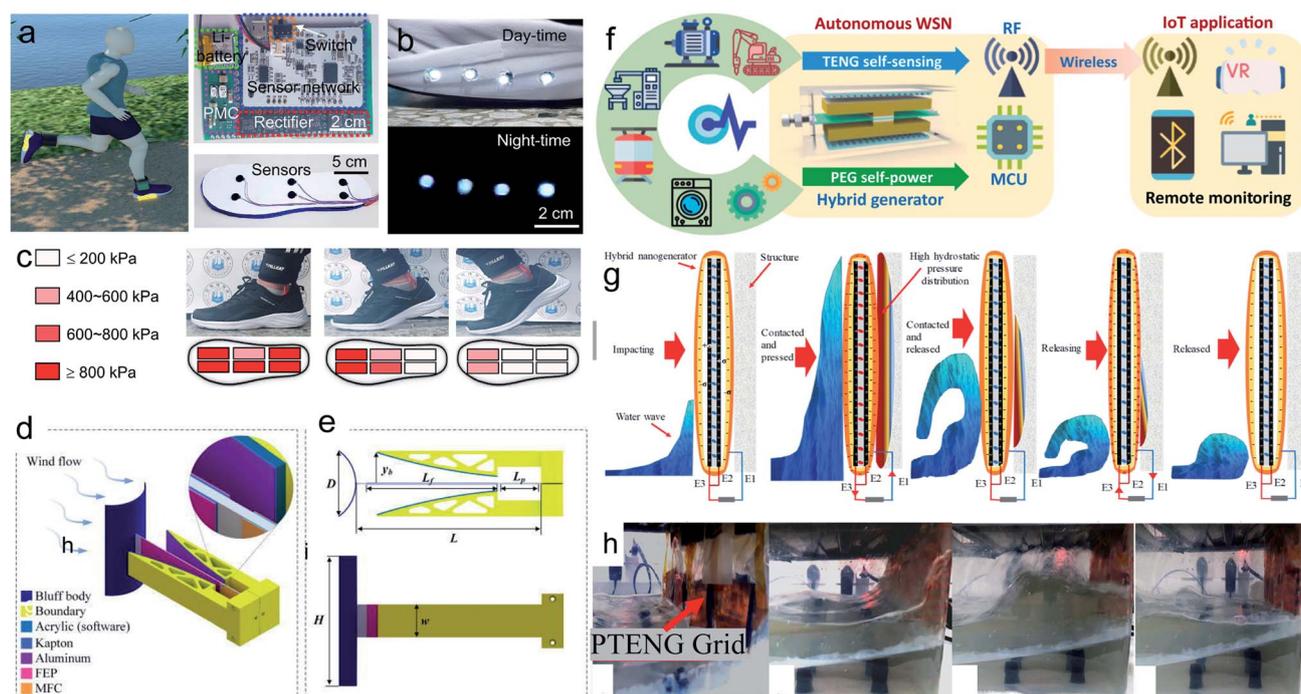

Fig. 12 Application of PTENGs at different scales. (a–c) PTENG powered LEDs in the shoe at different times of the day and foot pressure monitoring. (a) Self-powered lightning by walking and running; (b) LED embedded sole; (c) wireless foot pressure sensing. Reproduced with permission.[75] Copyright 2020, Elsevier. (d and e) Hybrid nanogenerator for small scale wind energy harvesting. (d) Cantilever device structure with various functional layers; (e) geometric configuration. Reproduced from ref. 73 with the permission of AIP Publishing. (f) Illustration graph of wireless sensing of equipment vibration by a PTENG. Reproduced with permission.[87] Copyright 2021, Elsevier. (g and h) Grid of PTENGs to harvest wave impact energy. (g) PTENG working mechanism under wave impact; (h) photos of the PTENG grid located on the wave tank wall before water impact, contacted and pressed, contacted and released, and releasing (from left to right). Reproduced with permission.[88] Copyright 2020, Elsevier.

demonstrated a virtual reality train monitoring system using a self-powered wireless sensing node constructed from hybrid PTENGs in harsh environments.[87] The transmitted acceleration signals were sent wirelessly presenting diverse potentials for IoT applications (Fig. 12f). The grids of PTENGs showed energy conversion efficiency as high as 30.22% for harvesting large scale water wave energy that is suitable for powering self-sustainable coastal wireless sensors (Fig. 12g and h).[88]

Challenges for future development of hybrid PTENGs and conclusion

All in all, hybrid PTENGs that combine piezoelectric and triboelectric mechanisms can increase energy scavenging and conversion efficiency beyond the linear summation of separate piezoelectric and triboelectric generators. By the rational design of the nano- and micro-structures and polarization directions, both mechanical deformation and contact friction of materials can be utilized simultaneously for energy scavenging.

There are still many challenges for the further development of hybrid PTENGs for their broader uses in practical applications. Power generation from nanogenerators is still low due to the low biomechanical energy and the small frequency of mechanical movement. Triboelectricity produces a high output voltage but low output current; sometimes the voltage can even be high enough to produce an arc between the two triboelectric layers, resulting in leakage, further reducing the nanogenerator power output.

It is imperative to continuously investigate the enhancement of the PTENG power output performance based on the coupling mechanisms between piezoelectric and triboelectric effects. Nanofillers such as lead-free inorganic compounds (e.g. BTO and KNN), metallic nanofillers, carbon nanofillers, and ionic salts are effective nucleating fillers to induce polar electroactive phases, with no requirement for electrical polarization, to achieve a higher piezoelectric effect and dielectric properties that facilitate electrical performance. These nanofillers are also able to increase the stretchability, flexibility and robustness of the fabricated nanogenerators.[18] With the introduction of these nanofillers, parameters such as charge transport, distribution in the polymer matrices and breakdown fields are significantly influenced, e.g. the breakdown strength of polymer/conductive filler nanocomposites can be modulated because of the high conductivity of nanofillers that can reversely alter the piezoelectricity. Strategies such as alignment of conductive fillers along with the perpendicular direction of the electric field can be implemented to improve the performance of PTENGs.[89] Further electrical polarization either by contact or non-contact modes (applying a corona discharge close to the specimens)/ionized air injection can also improve the electroactive phase content and enhance nanogenerator performance. Since the triboelectric effect is basically a surface charging process, to modify the tribosurface structure and morphology with micro- and nano-structure patterns (multiscale patterns,[90] and nanofeature surfaces such as pyramid patterns) can increase the roughness and effective friction area, resulting in an enhanced triboelectric effect and electrical outputs. Apart from surface structural variations, materials characteristics such as electron affinity and the work function also strongly affect the output performance.

In view of the potential applications of PTENGs as sensors in physiological monitoring and medical treatment, sensing sensitivity needs to be further honed towards self-powered sensors based on minute physiological signs such as heart beats, intestinal movement, and respiratory rates. Self-powered sensors are usually able to realize either a broad testing range or high sensitivity. For example, some of these sensors can offer high sensitivity when sensing human pulse waveforms but cannot accurately detect human motion since they have poor linearity (many of them are only useful for giving binary information) and a limited sensing range.[91] By using smart new material choices and a well-optimized compliant structure of hybrid PTENGs, the sensing intensity and relaxation time can be controlled and the sensitivity and accuracy can be improved to realize broad sensing ranges, better sensitivity and also wearing comfort. The capability to detect changes in pressure, motion and temperature provides wider uses for monitoring pulse, breathing and body temperature and also expands applications in medical treatment and athletic training.

Stability and durability are important factors in developing both self-powered sensors and energy harvesters. Under repetitive mechanical loading or strong chemical treatments, significant reduction in the electrical performance of PTENGs may occur due to the worn or destroyed surficial morphological micro/nano structures.[92] In real applications, PTENGs may be affected by various environmental factors such as humidity, dryness, high and low temperature, radiation, and adsorbed substances from surroundings, which are all distant from the reasonably controlled laboratory conditions. For instance, the contact electrification process for generating triboelectricity can be highly influenced by water absorption since water can fill the nano gaps or form as thin layers on surfaces during the operation, which strongly deteriorate the output performance, stability and durability of nanogenerators. Humidity can result in reduction in the dielectric strength of piezoelectric materials that affect ion and defect mobilities between grain boundaries and electrode materials. This further causes device failure due to increased power consumption as a result of the leaked current. Additional proposed causes for degraded performance from water include increased surface conduction, structural assimilation of interstitial atomic hydrogen and replaced oxygen vacancies through ceramics.[93] The negative influence of high temperature on piezoelectric properties is mainly because a ferroelectric material loses polarization above the Curie temperature; the triboelectric effect is also limited by temperature due to the electron thermion emission.[94] UV radiation affects electrical performance by desorbing oxygen molecules and therefore leads to a reduced piezoelectric effect. Contaminants such as absorbed substances change the resistance of functional materials and vary the leakage current of piezoelectric materials and influence the device performance.

More research is required in this aspect since being able to function outside of controlled environments is a prerequisite for long term sensing in a wide range of applications from those for home appliances to sophisticated outer space gadgets. High

quality packaging with special sealing techniques can be a way of solving this issue; however, such approaches will undoubtfully increase the complexity and fabrication cost. Hydrophobic surfaces are preferable since it is more difficult for water or moisture to transfer through them. PTENGs have similar issues to TENGs as they also need contact separation or sliding motion that cause damage by long term cyclic movements. Therefore, low durability affects the practical use of PTENGs for continuous health monitoring and needs to be addressed.

In addition to physiological monitoring of human activities, hybrid PTENGs have been manufactured into flapping-blade devices to harvest wind energy.[95] In such devices, the flexible piezoelectric cantilever converts wind energy to an electrical output and the flapping blades, attached with the cantilever, make contact with double frames at each side to amplify the vibration and friction, showing good performance in terms of power density at low wind speeds. Such energy harvesting systems should be further explored for industrial uptake. PTENG has also been made into self-charging energy storage packages to combine hybrid nanogenerators with electrochromic micro-supercapacitors, which can also show charging in real-time.[26] However, these intelligent systems require significant improvement in their conversion efficiency. Altogether, hybrid PTENGs have also been shown to harvest rotation mechanical energy effectively through movements from human activity, vehicles, wind, and waves.[85] All these features demonstrate that hybrid PTENGs are effective sustainable power resources that can contribute to both large energy harvesting platforms that can play an important role against the greenhouse effect, global warming and small digital healthcare devices for self-powered sensors for healthcare and sport training, and solving the issue of decentralized IoT devices in the future. This will further lead to three main trends in the outlook of smart cities through mass urbanization by incorporating intelligent devices, self-powered bioelectronics for personalized healthcare, and exploration of renewable energies for climate change and energy crisis

mitigations.[96] The challenges for future development of PTENGs are summarized in Fig. 13.

The fast-evolving information age requires highly efficient energy supply and wide ranges of solutions to power diverse intelligent devices and technologies for sensing, monitoring, interacting, and recognizing and learning. While large scale installation of sensors poses great challenges, hybrid piezo–triboelectric nanogenerators are low-cost, and accessible, enabling infrastructure for big data and artificial intelligence. PTENGs can be potentially applied in diverse areas such as intelligent sports, artificial sensory nervous systems, intelligent signal recognition, security systems and document management systems, etc.[97] For example, PTENG technology can bring many opportunities for intelligent athlete training and competition. Large amounts of distributed self-powered sensors and smart devices can be connected into a network that is able to measure movements of athletes and record exercise habits for future improvement in performance, with the facilitation from big data analysis and cloud computing.[98] In addition, artificial intelligence (AI) can assist with designing and improving the performance of PTENGs depending on the application requirements.[99] For the proliferation of self-powered sensors in large scale deployment, the cost of the current energy harvesting solutions needs to be reduced several orders of magnitude.[97]

In this review, we have analyzed the basic working principles, micro and nano-structure designs, manufacturing processes, performance enhancements, and applications of hybrid PTENGs. Combing the characteristics of piezoelectric materials and triboelectric generators, PTENGs offer a higher efficiency and broader energy collection frequency band than either piezoelectric and triboelectric systems. Due to the coupling effect, the electrical output of PTENGs is more than the simple addition of the triboelectric and the piezoelectric parts, stemming from the synergistic enhancement between the two mechanisms. PTENGs also have a versatile designing architecture to meet different practical needs.
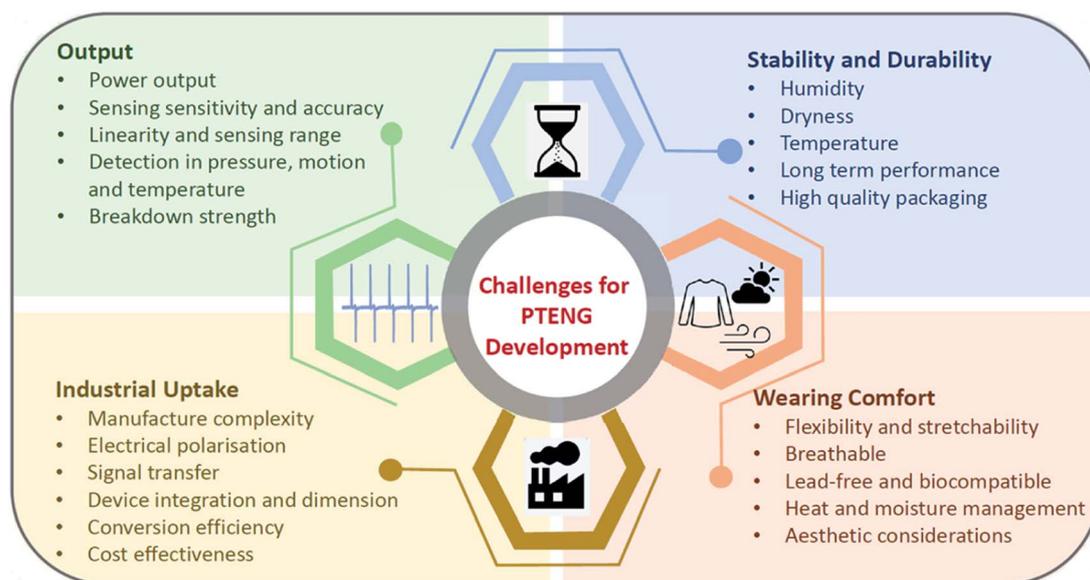

Fig. 13 Summary of challenges for the future development of PTENG.

Innovative electrode structures should be used to simplify production complexity, ease signal transfer and reduce device dimensions. Further challenges such as improvement of stability and durability remain to achieve broader practical applications. New materials, designs and optimization approaches are required to address these challenges so that PTENGs can be envisioned for physiological monitoring, health care, transportation, marine energy, and smart city applications.

Conflicts of interest

There are no conflicts to declare.

References

1 Y. Hu and Z. L. Wang, *Nano Energy*, 2015, **14**, 3–14.

2 W. Paosangthong, R. Torah and S. Beeby, *Nano Energy*, 2019, **55**, 401–423.

3 P. Glynne-Jones, S. P. Beeby and N. M. White, *IEE Proc.: Sci., Meas. Technol.*, 2001, **148**, 68–72.

4 Z. L. Wang and J. Song, *Science*, 2006, **312**, 242–246.

5 F.-R. Fan, Z.-Q. Tian and Z. Lin Wang, *Nano Energy*, 2012, **1**, 328–334.

6 G. Zhu, Z. H. Lin, Q. Jing, P. Bai, C. Pan, Y. Yang, Y. Zhou and Z. L. Wang, *Nano Lett.*, 2013, **13**, 847–853.

7 S. R. Anton and H. A. Sodano, *Smart Mater. Struct.*, 2007, **16**, R1–R21.

8 X. Guan, B. Xu and J. Gong, *Nano Energy*, 2020, **70**, 104516.

9 J. Xing, H. Chen, L. Jiang, C. Zhao, Z. Tan, Y. Huang, B. Wu, Q. Chen, D. Xiao and J. Zhu, *Nano Energy*, 2021, **84**, 105900.

10 X. Guan, H. Chen, H. Xia, Y. Fu, J. Yao and Q.-Q. Ni, *Composites, Part B*, 2020, **197**, 108169.

11 M. A. Johar, A. Waseem, M. A. Hassan, I. V. Bagal, A. Abdullah, J.-S. Ha and S.-W. Ryu, *Adv. Energy Mater.*, 2020, **10**, 2002608.

12 N.-J. Ku, G. Liu, C.-H. Wang, K. Gupta, W.-S. Liao, D. Ban and C.-P. Liu, *Nanoscale*, 2017, **9**, 14039–14046.

13 H. Khan, N. Mahmood, A. Zavabeti, A. Elbourne, M. A. Rahman, B. Y. Zhang, V. Krishnamurthi, P. Atkin, M. B. Ghasemian, J. Yang, G. Zheng, A. R. Ravindran, S. Walia, L. Wang, S. P. Russo, T. Daeneke, Y. Li and K. Kalantar-Zadeh, *Nat. Commun.*, 2020, **11**, 3449.

14 X. Song, F. Hui, K. Gilmore, B. Wang, G. Jing, Z. Fan, E. Grustan-Gutierrez, Y. Shi, L. Lombardi, S. A. Hodge, A. C. Ferrari and M. Lanza, *Nanoscale*, 2017, **9**, 6237–6245.

15 Z. L. Wang, *ACS Nano*, 2013, **7**, 9533.

16 Q. Jiang, B. Chen, K. Zhang and Y. Yang, *ACS Appl. Mater. Interfaces*, 2017, **9**, 43716–43723.

17 X. Peng, K. Dong, C. Ye, Y. Jiang, S. Zhai, R. Cheng, D. Liu, X. Gao, J. Wang and Z. L. Wang, *Sci. Adv.*, 2020, **6**, eaba9624.

18 J. Zhang, D. Liu, Q. Han, L. Jiang, H. Shao, B. Tang, W. Lei, T. Lin and C. H. Wang, *Composites, Part B*, 2019, **175**, 107157.

19 G. Khandelwal, A. Chandrasekhar, N. P. Maria Joseph Raj and S.-J. Kim, *Adv. Energy Mater.*, 2019, **9**, 1803581.

20 L. Lan, T. Yin, C. Jiang, X. Li, Y. Yao, Z. Wang, S. Qu, Z. Ye, J. Ping and Y. Ying, *Nano Energy*, 2019, **62**, 319–328.

21 Y. Liu, J. Ping and Y. Ying, *Adv. Funct. Mater.*, 2021, **31**, 2009994.

22 S. Chandrasekaran, C. Bowen, J. Roscow, Y. Zhang, D. K. Dang, E. J. Kim, R. D. K. Misra, L. Deng, J. S. Chung and S. H. Hur, *Phys. Rep.*, 2019, **792**, 1–33.

23 X. Feng, H. Zou, H. Xiang, X. Guo, T. Zhou, Y. Wu, W. Xu, P. Yan, C. Wang, J. G. Zhang and Y. Yu, *ACS Appl. Mater. Interfaces*, 2016, **8**, 16718–16726.

24 Y.-K. Fuh, S.-C. Li and C.-Y. Chen, *APL Mater.*, 2017, **5**, 074202.

25 J. Chen, H. Guo, X. He, G. Liu, Y. Xi, H. Shi and C. Hu, *ACS Appl. Mater. Interfaces*, 2016, **8**, 736–744.

26 S. Qin, Q. Zhang, X. Yang, M. Liu, Q. Sun and Z. L. Wang, *Adv. Energy Mater.*, 2018, **8**, 1800069.

27 J. He, S. Qian, X. Niu, N. Zhang, J. Qian, X. Hou, J. Mu, W. Geng and X. Chou, *Nano Energy*, 2019, **64**, 103933.

28 J. Song, B. Yang, W. Zeng, Z. Peng, S. Lin, J. Li and X. Tao, *Adv. Mater. Technol.*, 2018, **3**, 1800016.

29 S. Chen, X. Tao, W. Zeng, B. Yang and S. Shang, *Adv. Energy Mater.*, 2017, **7**, 1601569.

30 P. Sahatiya, S. Kannan and S. Badhulika, *Applied Materials Today*, 2018, **13**, 91–99.

31 D. W. Lee, D. G. Jeong, J. H. Kim, H. S. Kim, G. Murillo, G.-H. Lee, H.-C. Song and J. H. Jung, *Nano Energy*, 2020, **76**, 105066.

32 W. S. Jung, M. G. Kang, H. G. Moon, S. H. Baek, S. J. Yoon, Z. L. Wang, S. W. Kim and C. Y. Kang, *Sci. Rep.*, 2015, **5**, 9309.

33 H. H. Singh and N. Khare, *Nano Energy*, 2018, **51**, 216–222.

34 Q. Zhu, L. Dong, J. Zhang, K. Xu, Y. Zhang, H. Shi, H. Lu, Y. Wu, H. Zheng and Z. Wang, *Ceram. Int.*, 2020, **46**, 28277–28284.

35 G. Suo, Y. Yu, Z. Zhang, S. Wang, P. Zhao, J. Li and X. Wang, *ACS Appl. Mater. Interfaces*, 2016, **8**, 34335–34341.

36 Y. Qian and D. J. Kang, *ACS Appl. Mater. Interfaces*, 2018, **10**, 32281–32288.

37 S. Pongampai, T. Charoonsuk, N. Pinpru, P. Pulphol, W. Vittayakorn, P. Pakawanit and N. Vittayakorn, *Composites, Part B*, 2021, **208**, 108602.

38 T. Huang, C. Wang, H. Yu, H. Wang, Q. Zhang and M. Zhu, *Nano Energy*, 2015, **14**, 226–235.

39 D. H. Kim, B. Dudem and J. S. Yu, *ACS Sustainable Chem. Eng.*, 2018, **6**, 8525–8535.

40 H. Patnam, B. Dudem, N. R. Alluri, A. R. Mule, S. A. Graham, S.-J. Kim and J. S. Yu, *Compos. Sci. Technol.*, 2020, **188**, 107963.

41 M. Sahu, V. Vivekananthan, S. Hajra, D. K. Khatua and S.-J. Kim, *Applied Materials Today*, 2021, **22**, 100900.

42 Y. Wu, J. Qu, W. A. Daoud, L. Wang and T. Qi, *J. Mater. Chem. A*, 2019, **7**, 13347–13355.

43 W. Wang, J. Zhang, Y. Zhang, F. Chen, H. Wang, M. Wu, H. Li, Q. Zhu, H. Zheng and R. Zhang, *Appl. Phys. Lett.*, 2020, **116**, 023901.

44 G. Hassan, F. Khan, A. Hassan, S. Ali, J. Bae and C. H. Lee, *Nanotechnology*, 2017, **28**, 175402.

45 X.-S. Z. Mengdi Han, B. Meng, W. Liu, W. Tang, X. Sun, W. Wang and H. Zhang, *ACS Nano*, 2013, **7**, 8554–8560.

46 S. Cheon, H. Kang, H. Kim, Y. Son, J. Y. Lee, H.-J. Shin, S.-W. Kim and J. H. Cho, *Adv. Funct. Mater.*, 2018, **28**, 1703778.

47 Y. M. Yousry, K. Yao, A. M. Mohamed, W. H. Liew, S. Chen and S. Ramakrishna, *Adv. Funct. Mater.*, 2020, **30**, 1910592.

48 A. A. Narasimulu, P. Zhao, N. Soin, K. Prashanthi, P. Ding, J. Chen, S. Dong, L. Chen, E. Zhou, C. D. Montemagno and J. Luo, *Nano Energy*, 2017, **40**, 471–480.

49 S. H. Ji, W. Lee and J. S. Yun, *ACS Appl. Mater. Interfaces*, 2020, **12**, 18609–18616.

50 T. Huang, Y. Zhang, P. He, G. Wang, X. Xia, G. Ding and T. H. Tao, *Adv. Mater.*, 2020, **32**, e1907336.

51 X. Tao, H. Jin, M. Ma, L. Quan, J. Chen, S. Dong, H. Zhang, C. Lv, Y. Fu and J. Luo, *Phys. Status Solidi A*, 2019, **216**, 1900068.

52 S. Sriphan, T. Charoonsuk, T. Maluangnont and N. Vittayakorn, *ACS Appl. Energy Mater.*, 2019, **2**, 3840–3850.

53 S. Niu and Z. L. Wang, *Nano Energy*, 2015, **14**, 161–192.

54 C. Xue, J. Li, Q. Zhang, Z. Zhang, Z. Hai, L. Gao, R. Feng, J. Tang, J. Liu, W. Zhang and D. Sun, *Nanomaterials*, 2014, **5**, 36–46.

55 J. Zhu, X. Hou, X. Niu, X. Guo, J. Zhang, J. He, T. Guo, X. Chou, C. Xue and W. Zhang, *Sens. Actuators, A*, 2017, **263**, 317–325.

56 J. Zhang, M. Shi, H. Chen, M. Han, Y. Song, X. Cheng and H. Zhang, *presented in part at the 2016 IEEE 29th International Conference on Micro Electro Mechanical Systems (MEMS)*, 2016, pp. 173–176.

57 S. C. Mannsfeld, B. C. Tee, R. M. Stoltenberg, C. V. Chen, S. Barman, B. V. Muir, A. N. Sokolov, C. Reese and Z. Bao, *Nat. Mater.*, 2010, **9**, 859–864.

58 A. Yu, Y. Zhu, W. Wang and J. Zhai, *Adv. Funct. Mater.*, 2019, **29**, 1900098.

59 Y. Zou, J. Xu, K. Chen and J. Chen, *Adv. Mater. Technol.*, 2021, **6**, 2000916.

60 M. Li, Y. Jie, L.-H. Shao, Y. Guo, X. Cao, N. Wang and Z. L. Wang, *Nano Res.*, 2019, **12**, 1831–1835.

61 A. R. Chowdhury, A. M. Abdullah, I. Hussain, J. Lopez, D. Cantu, S. K. Gupta, Y. Mao, S. Danti and M. J. Uddin, *Nano Energy*, 2019, **61**, 327–336.

62 X. Yang and W. A. Daoud, *Adv. Funct. Mater.*, 2016, **26**, 8194–8201.

63 X. Yang and W. A. Daoud, *J. Mater. Chem. A*, 2017, **5**, 9113–9121.

64 B. Dudem, D. H. Kim, L. K. Bharat and J. S. Yu, *Appl. Energy*, 2018, **230**, 865–874.

65 M. M. Abolhasani, K. Shirvanimoghaddam and M. Naebe, *Compos. Sci. Technol.*, 2017, **138**, 49–56.

66 J. Yu, X. Yang and Q. Sun, *Advanced Intelligent Systems*, 2020, **2**, 1900175.

67 Y. Guo, X.-S. Zhang, Y. Wang, W. Gong, Q. Zhang, H. Wang and J. Brugger, *Nano Energy*, 2018, **48**, 152–160.

68 L. Wang, T. He, Z. Zhang, L. Zhao, C. Lee, G. Luo, Q. Mao, P. Yang, Q. Lin, X. Li, R. Maeda and Z. Jiang, *Nano Energy*, 2021, **80**, 105555.

69 J. Yu, X. Hou, M. Cui, S. Zhang, J. He, W. Geng, J. Mu and X. Chou, *Nano Energy*, 2019, **64**, 103923.

70 M. Zhu, Q. Shi, T. He, Z. Yi, Y. Ma, B. Yang, T. Chen and C. Lee, *ACS Nano*, 2019, **13**, 1940–1952.

71 L. Bu, Z. Chen, Z. Chen, L. Qin, F. Yang, K. Xu, J. Han and X. Wang, *Nano Energy*, 2020, **70**, 104500.

72 X. Chen, M. Han, H. Chen, X. Cheng, Y. Song, Z. Su, Y. Jiang and H. Zhang, *Nanoscale*, 2017, **9**, 1263–1270.

73 Q. Wang, H.-X. Zou, L.-C. Zhao, M. Li, K.-X. Wei, L.-P. Huang and W.-M. Zhang, *Appl. Phys. Lett.*, 2020, **117**, 043902.

74 X. Yu, X. Liang, R. Krishnamoorthy, W. Jiang, L. Zhang, L. Ma, P. Zhu, Y. Hu, R. Sun and C.-P. Wong, *Smart Mater. Struct.*, 2020, **29**, 045040.

75 D. W. Lee, D. G. Jeong, J. H. Kim, H. S. Kim, G. Murillo, G.-H. Lee, H.-C. Song and J. H. Jung, *Nano Energy*, 2020, **76**, 105066.

76 W. Yang, W. Gong, C. Hou, Y. Su, Y. Guo, W. Zhang, Y. Li, Q. Zhang and H. Wang, *Nat. Commun.*, 2019, **10**, 5541.

77 X. Fan, J. Chen, J. Yang, P. Bai, Z. Li and Z. L. Wang, *ACS Nano*, 2015, **9**, 4236–4243.

78 N. Cui, L. Gu, J. Liu, S. Bai, J. Qiu, J. Fu, X. Kou, H. Liu, Y. Qin and Z. L. Wang, *Nano Energy*, 2015, **15**, 321–328.

79 F. Wen, T. He, H. Liu, H.-Y. Chen, T. Zhang and C. Lee, *Nano Energy*, 2020, **78**, 105155.

80 K. Shi, X. Huang, B. Sun, Z. Wu, J. He and P. Jiang, *Nano Energy*, 2019, **57**, 450–458.

81 P. Manchi, S. A. Graham, B. Dudem, H. Patnam and J. S. Yu, *Compos. Sci. Technol.*, 2021, **201**, 108540.

82 Z. S. Minglu Zhu, Z. Zhang, Q. Shi, T. He, H. Liu, T. Chen and C. Lee, *Sci. Adv.*, 2020, **6**, eaaz8693.

83 Y. Su, X. Wen, G. Zhu, J. Yang, J. Chen, P. Bai, Z. Wu, Y. Jiang and Z. Lin Wang, *Nano Energy*, 2014, **9**, 186–195.

84 N. R. Alluri, A. Chandrasekhar and S.-J. Kim, *ACS Sustainable Chem. Eng.*, 2018, **6**, 1919–1933.

85 C. Zhao, Q. Zhang, W. Zhang, X. Du, Y. Zhang, S. Gong, K. Ren, Q. Sun and Z. L. Wang, *Nano Energy*, 2019, **57**, 440–449.

86 Z. Li, Z. Saadatnia, Z. Yang and H. Naguib, *Energy Convers. Manage.*, 2018, **174**, 188–197.

87 L. Wang, T. He, Z. Zhang, L. Zhao, C. Lee, G. Luo, Q. Mao, P. Yang, Q. Lin, X. Li, R. Maeda and Z. Jiang, *Nano Energy*, 2021, **80**, 105555.

88 U. T. Jurado, S. H. Pu and N. M. White, *Nano Energy*, 2020, **72**, 104701.

89 L. Yang, H. Ji, K. Zhu, J. Wang and J. Qiu, *Compos. Sci. Technol.*, 2016, **123**, 259–267.

90 Z. Fang, K. H. Chan, X. Lu, C. F. Tan and G. W. Ho, *J. Mater. Chem. A*, 2018, **6**, 52–57.

91 J. Yu, X. Hou, M. Cui, S. Zhang, J. He, W. Geng, J. Mu and X. Chou, *Nano Energy*, 2019, **64**, 103923.

92 K. Dong, X. Peng and Z. L. Wang, *Adv. Mater.*, 2020, **32**, 1902549.

93 L. Chen, X. M. Xiong, H. Meng, P. Lv and J. X. Zhang, *Appl. Phys. Lett.*, 2006, **89**, 071916.

94 C. X. Lu, C. B. Han, G. Q. Gu, J. Chen, Z. W. Yang, T. Jiang, C. He and Z. L. Wang, *Adv. Eng. Mater.*, 2017, **19**, 1700275.

95 T. Chen, Y. Xia, W. Liu, H. Liu, L. Sun and C. Lee, *J. Microelectromech. Syst.*, 2016, **25**, 845–847.

96 X. Zhao, H. Askari and J. Chen, *Joule*, 2021, **5**, 1391–1431.

97 Y. Zhou, M. Shen, X. Cui, Y. Shao, L. Li and Y. Zhang, *Nano Energy*, 2021, **84**, 105887.

98 J. Luo, W. Gao and Z. L. Wang, *Adv. Mater.*, 2021, **33**, 2004178.

99 P. Jiao, *Nano Energy*, 2021, **88**, 106227.